

Wright State University

CORE Scholar

---

[Browse all Theses and Dissertations](#)

[Theses and Dissertations](#)

---

2013

## Wing Damage Effect on Dragonfly's Aerodynamic Performance during Takeoff

Kuo Gai

*Wright State University*

Follow this and additional works at: [https://corescholar.libraries.wright.edu/etd\\_all](https://corescholar.libraries.wright.edu/etd_all)



Part of the [Mechanical Engineering Commons](#)

---

### Repository Citation

Gai, Kuo, "Wing Damage Effect on Dragonfly's Aerodynamic Performance during Takeoff" (2013). *Browse all Theses and Dissertations*. 813.

[https://corescholar.libraries.wright.edu/etd\\_all/813](https://corescholar.libraries.wright.edu/etd_all/813)

This Thesis is brought to you for free and open access by the Theses and Dissertations at CORE Scholar. It has been accepted for inclusion in Browse all Theses and Dissertations by an authorized administrator of CORE Scholar. For more information, please contact [library-corescholar@wright.edu](mailto:library-corescholar@wright.edu).

# **Wing Damage Effect on Dragonfly's Aerodynamic Performance during Takeoff**

A thesis submitted in partial fulfillment of the  
requirements for the degree of Master  
of Science in Engineering

By

Kuo Gai  
B.S., Dalian Jiaotong University, 2010

2013  
Wright State University

WRIGHT STATE UNIVERSITY

GRADUATE SCHOOL

June 20,2012

I HEREBY RECOMMEND THAT THE THESIS PREPARED UNDER MY SUPERVISION  
BY Kuo Gai ENTITLED Wing Damage Effect on Dragonfly's Aerodynamic Performance during  
Takeoff BE ACCEPTED IN PARTIAL FULFILLMENT OF THE REQUIREMENTS FOR THE  
DEGREE OF Master of Science in Engineering.

---

Haibo Dong, Ph.D.

Thesis Director

---

George Huang, Ph.D., Chair

Department of Mechanical and Materials Engineering

College of Engineering and Computer Science

Committee on

Final Examination

---

Haibo Dong, Ph.D.

---

Zifeng Yang, Ph.D.

---

Hui Wan, Ph.D.

---

Andrew Hsu, Ph.D.

Dean, School of Graduate Studies

## ABSTRACT

Gai, Kuo. M.S. Egr., Department of Mechanical and Material Engineering, Wright State University, 2013. Wing Damage Effect on Dragonfly's Aerodynamic Performance during Takeoff.

Insect wing damage resulted from living environment or predation commonly happens in nature. This usually results in deterioration of insect's flight performance and as a consequence, the insect needs adjustment of flapping wings to compensate the effect from the wing loss. In this study, a dragonfly (*Erythemis simpliciolis*) with and without wing loss is chosen to study the change of aerodynamic performance of flapping wings. Three cases including flight with intact wings (IW), flight with one-sided forewing damage (OFD), and flight with double-side forewing damage (DFD) are determined. An integrated study using high-speed photogrammetry, three-dimensional surface reconstruction, and direct numerical simulation (DNS) are used to quantify wing kinematics and aerodynamics performance. Results have shown that in general, during downstroke of forewings, forewing area loss could reduce insect's lift production; The lift force generated by the outer wings is larger than or equal to that produced by the inner wings during downstroke, but the outer wings' lift production becomes smaller than the inner wings' during upstroke; Span-wise forewing area removal reduces forewing tip vorticity, and it leads to the detachment of the tip vortex ring during upstroke.

## TABLE OF CONTENTS

	Page
I. INTRODUCTION .....	1
II. METHODS .....	6
1: Experiment Setup .....	6
1.1: 3D High speed photogrammetry system .....	6
1.2: 3D Surface Reconstruction technology--Autodesk MAYA .....	7
2: Design of Wing-Damage Experiment .....	9
2.1: Species of Dragonfly and Environment in laboratory .....	9
2.2: Implementation of Experiment .....	10
3: Coordinate Transformation .....	14
4: Direct Numerical Simulation method (DNS) .....	16
III. RESUTLS AND DISCUSSIONS .....	18
1: Morphological parameters .....	18
2: Mean Wing beat frequency .....	19
3: Displacement of the dragonfly's body .....	19
4: Lift performance .....	21
4.1: Resultant Lift .....	21
4.2: Lift on individual wings .....	24
5: Left hindwing kinematics .....	34
6: Flow features .....	36
IV. CONCLUSIONS .....	51
V. FUTURE WORK .....	53
REFERENCES .....	54

## LIST OF FIGURES

Figure	Page
1. 3D High speed photogrammetry system. Camera. ....	6
2. Reconstructed model built by Autodesk MAYA. ....	8
3. Three dimensional surface reconstruction. ....	9
4. One studied dragonfly with artificial markers and the damaged area on the forewings. ....	11
5. Motion in different time of the three cases filmed by 3D High speed photogrammetry system. ....	14
6. Global Cartesian coordinate in reconstruction system. ....	14
7. Local coordinate system when investigating wing kinematics. ....	15
8. Validation case. ....	17
9. Time history of displacement in three directions. ....	20
10. Instantaneous lift generated by the individual's four wings during 0.08s. ....	22
11. Lift for four wings versus time in one completed stroke. ....	30
12. Trajectory of mid chord of the left hindwing and the corresponding instantaneous pitching angle in the IW and OFD cases. ....	35
13. Flow Feature shed from the intact wings during 0.08s (the IW case). Iso-surface of vorticity $\lambda_2$ is 3. ....	37
14. Flow Feature shed from the dragonfly's wings including 40% loss of left forewing area during 0.08s (the OFD case). Iso-surface of vorticity $\lambda_2$ is 3. ....	39

15. Flow Feature shed from the dragonfly's wings including 40% loss of wing area on the two forewings during 0.08s. ....	40
16. YZ view (side view) of the three cases.. ....	41
17. Flow feature of the intact wings in the IW case.. ....	43
18. Flow feature of four wings including damaged left forewing in the OFD case. ....	45
19. Flow feature of the four wings in the DFD case. ....	48
20. Comparison of the vorticity slice of the inner forewing at the end of downstroke....	49

## LIST OF TABLES

Table	Page
1. Flying motion of the dragonfly in the three cases.....	12
2. Morphological parameters of the individual.....	18
3. Mean wing beating frequencies of four wings in the three cases .....	19
4. Mean lift on the four wings and the percentage of the mean lift on each wing for the downstroke and upstroke in the IW case. ....	25
5. Mean lift on the four wings and the percentage of the mean lift on each wing for the downstroke and upstroke in the OFD case. ....	25
6. Mean lift on the four wings and the percentage of the mean lift on each wing for the downstroke and upstroke in the DFD case. ....	26
7. Mean lift on the four wings and the percentage of the mean lift on each wing for the following downstroke of the one stroke studied in the IW, OFD, and DFD cases.....	26
8. Mean lift, average vertical acceleration computed from Newton's second law, $a$ , and average vertical acceleration computed from displacement and velocity, $a_k$ , in one stroke.....	34



## **ACKNOWLEDGEMENTS**

First of all, I want to thank Dr. Haibo Dong for all of his help, time, and funding support spending on my research work. Without these, I cannot finish my thesis. I am very luck to join his team and work under his direction. He used a lot of time to teach and guide me to do research. Whenever or whatever I needed his help on my study work and research work, he was always there and helped me. His encouragement and suggestion gave me a lot of confidence to let me finish my work. He helped me to open a new interesting field I never touched it before. Under his influence, I know how to study, and how to be a researcher. I really appreciate and I can bring all these skills into my future work and life. I also like to thank Dr. Hui Wan, post doctor in Dr. Dong's group. Thanks for his time and patient. He taught me a lot of skills when I met trouble in work, and also introduced a lot of useful books and papers to help my research work. Without his help, I cannot finish the work so fast and so nice.

Last but not least I would like to thank my family and all the members in Flow Simulation Research Group. Thanks for their time, help, and encouragement during my work. Especially, I like to thank Yan Ren for teaching me how to use Maya, how to use our in-house code. I really appreciate his time and help. At last, I would also like to thank Zhe Ning for his encouragement, understanding, and cooking. He gave me a lot of hints over last one year. Sometimes, these hits can help me save several day times. I do not think I can finish this work without him.

## I. INTRODUCTION

Dragonflies are ancient and excellent flyers with paired wings. They have fast and flexible maneuverability to capture their prey, adapt to harsh environment, and mate with each other. All of these are implemented by the clap and beating of two paired wings. Thus, the study on dragonflies' wing kinematics and aerodynamics has always been a popular research topic, especially because this could help in the improvement and accomplishment of bio-inspired micro air vehicle (MAV) design. In addition, during the life cycle of dragonflies, the wing damage resulting from living environment or predation commonly happens in nature, and this loss of wing area would absolutely influence their flying motion. Studying the effect of this phenomenon will give better understanding on dragonflies' flight and will also provide significant data for improving MAV design.

To investigate the aerodynamic performance of insects, many approaches were introduced to measure mean force or instantaneous force generated by insects' wings. A very common method is called quasi-steady method which can obtain mean lift and mean drag on insects' wings by quasi-steady assumption. However, Sane and Dickinson (2001) claim that this method can only perform better at translational predictions at high stroke amplitude rather than at lower stroke amplitude, and wing rotation would influence the estimation of force. Also, although the mean lift coefficient can be estimated accurately, the mean drag coefficient is underestimated. The reason of this underestimation is that the quasi-steady prediction cannot involve the effect from wing rotation.

A variety of methods were invented and utilized, but it was hard to obtain accurate solutions. Therefore, indirect measurement on aerodynamics was considered. A very popular approach using computational fluid dynamics (CFD) computes the flow field around insects by solving Navier-Stokes Equation to obtain forces produced by insects' wings. An accurate CFD solver used in this field is developed by Mittal and Dong (2008), et al. They use a sharp interface immersed boundary method and ghost-cell methodology to handle complicated three-dimensional stationary and moving body surfaces which are composed of unstructured tri-angular elements. Also, this solver uses non-uniform Cartesian grids and can simulate incompressible viscous flow when the region of Reynolds number is from  $O(10^1)$  to  $O(10^3)$ . In addition, Mittal and Dong, et al. tested and verified the accuracy of the solver using several canonical two- and three-dimensional flows and accelerated objects.

However, even if many accurate methods and solvers are provided to analyze aerodynamics performance and to estimate mean and instantaneous force on insects' bodies, it is still very complicated to study and analyze the relationship between wing kinematics and aerodynamics. The reason is that insects' flying motion including pitching, rolling, and yawing is random and complex, and wing motion and deformation including twisting, bending, and camber are also hard to be investigated separately. Thus, a rigid wing model was introduced in this field to study such fundamental phenomenon. Dickinson and Göze (1993) measured lift and drag and visualized flow based on a two-dimensional model wing, which moves from repose to a constant velocity after giving a sharp acceleration at a fixed angle of attack. They also claimed that the study tried to fill the lack of the data about time-dependent unsteady aerodynamic forces produced by

insects' wings when Reynolds number is from 10 to 1000. Also, Sane and Dickinson (2001) examined the relationship between wing kinematics and unsteady aerodynamic forces using a dynamically scaled mechanical model of fruit fly. They found that the magnitude of stroke deviation would influence the aerodynamic performance negatively, yet it might help insects transform forces amongst the wings to produce corresponding moments during maneuvering.

While two-dimensional wing models have been used to analyze and solve wing kinematics and aerodynamic performance, investigating aerodynamics of real insects' flight was in process simultaneously by Ellington et al. (Ellington, 1984a; Ellington, 1984b; Ellington, 1984c; Ellington, 1984d). Wakeling and Ellington (1997) examined mean lift coefficient, maximum muscle mass-specific power, which is approximately equivalent to the aerodynamic power, and heat production for the free flight of a dragonfly (*Sympetrum sanguineum*) and a damselfly (*Calopteryx splendens*). The results showed that owing to the characteristic of wings, the damselfly has bigger mean lift coefficient and higher muscle mass-specific power than the dragonfly when the velocity and the thrust were fixed, but the mechanical efficiency which is directly resulted from heat production performed in an opposite way for the two species.

In addition, many other species of insects were studied such as hawkmoth, locust, and bumblebees, etc. For example, Aono, Liang and Liu (2007) presented the study of vorticity, lift and drag, and torques on hovering flight of a fruit fly *Drosophila melanogaster*. They used a biology-inspired, dynamic flight simulator based on computational fluid dynamics to handle the realistic reconstructed model. The results involved the variation of vortices around the wings, the mean force, the instantaneous lift

and drag, time history of inertial torques and powers during one stroke. They finally concluded that according to the analysis of vortices, 62% of total lift generated in one stroke was produced in the upstroke, where the corresponding downwash was grossly stronger.

Nowadays, although there is much unknown knowledge on insects in free flight, the existing research and study provide better understanding about their motion. With the ongoing research on development of micro air vehicle design, the effect of damaged wings on aerodynamics becomes the focus. Combes and Mukherjee (2010) investigated the effect of hindwing area loss on dragonfly flight by linking laboratory and greenhouse experiments. They declared that the dragonflies with 30 percent loss of hindwing area resulted in an approximate 30 percent drop on vertical acceleration; when the loss of hindwing area was increased to 50 percent, the vertical acceleration decreased by nearly 50 percent. In addition, the maximum acceleration, the time-averaged velocity, and the escape velocity of dragonflies would be reduced with the increase of hindwing area loss. For example, when the hindwing area was removed 30 percent, the escape velocity dropped by 21 percent; while the loss of wing was increased to 50 percent, the velocity decreased by 24.8 percent.

However, there is less insight into the influence of wing damage on aerodynamic performance. Most literature on insect wing damage and wing wear is concentrated in the effect on predation, which is usually reported by biologists (Cartar, 1992; Dukas et al., 2011; Foster et al., 2011).

In this thesis, in order to investigate the effect of wing damage on aerodynamics, three cases from one dragonfly were studied, including flight with intact wings (IW), with one-sided forewing damage (OFD), and with double-side forewing damage (DFD). The flying motion in all these three cases are non-interference takeoff maneuvers. The three-dimensional realistic reconstructed model and in-house solver, *PiCar3D* using a sharp interface immersed boundary method and a multi-dimensional ghost-cell methodology, were utilized to compute aerodynamics performance including vortices and lift forces. Morphological parameters including mass, wing chord and span length were measured during these experiments. Also, the frequencies of the dragonfly's wings were examined individually before and after the wing area removal. The results involved the time-averaged lift over a half stroke, time history of lift during one stroke, resultant lift during takeoff motion, and the comparison of vortices around the wings. However, we need to measure wing kinematics and examine the relation between wing kinematics and aerodynamic performance on dragonflies' takeoff maneuver.

## II. METHODS

### 1: Experiment Setup

#### 1.1: 3D High speed photogrammetry system

The photogrammetry system used in collecting the images of insects' free flight in our laboratory is shown in Figure 1. It includes three synchronized Photron FASTCAM SA3 60K high-speed cameras with  $1024 \times 1024$  pixel resolution. In order to obtain exact three-dimensional data of insects' motion, the three cameras are placed orthogonal to each other. They are operated at 1000 Hz and have a  $1/20000$  sec. shutter speed, so the time-step size is 0.001s. All the three cameras are controlled by a delayed controller that can make the memory in cameras store previous two seconds images.

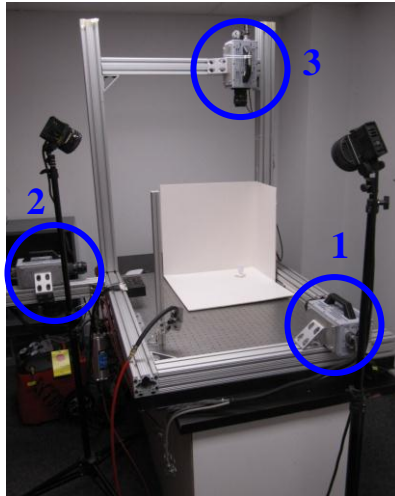


Figure 1 3D High speed photogrammetry system. Camera No.1 films the side-view images, Camera No.2 films the front-view images, and Camera No.3 films the top-view images.

Also, the filming domain is illuminated by 2 optic lamps (OSRAM, 54428) to supply enough light for the fast shutter speed mentioned above. Each camera is set at a distance of 85cm from the initial position of insects to ensure filming of the completed takeoff motion of dragonflies. The images filmed by the three cameras are shown in Figure 3.

### 1.2: 3D Surface Reconstruction technology--Autodesk MAYA

The foundation required to analyze free flight of a dragonfly is the acquisition of the displacement of every single point on dragonfly's body and the wings. The information of displacement is supposed to be with respect to global Cartesian coordinate system. One goal to get more detailed and accurate information of body and wings is to create a model which has as many points as possible on their surfaces within the valid region of computation. Then using this data of the displacement measured we can calculate the related kinematics and aerodynamics.

In order to achieve the goal mentioned above to build a 3D model based on the photographs filmed by the photogrammetry system in Figure 1, Autodesk MAYA software is selected. The model created using this software is shown in Figure 2. The model of a dragonfly's body is built by Catmull-Clark subdivision surfaces corresponding to two pictures of real dragonfly in side and top view. The exact profile of body is generated by modifying the position of control points on the model surface. Since dragonfly's wings are treated as membrane which does not have thickness, NURBS surfaces are chosen, and the control points on the surfaces should track the corresponding marker on real wings, as shown in Figure 2 a). The reason why only the points on edges



of wings are tracked is to simplify the deformation of a dragonfly's wings by assuming the wings are rigid. However, if the deformation during flight is considered important in future work, it is easy to add one more line in the mid span of each wing to track the corresponding markers then generate the camber of wings.

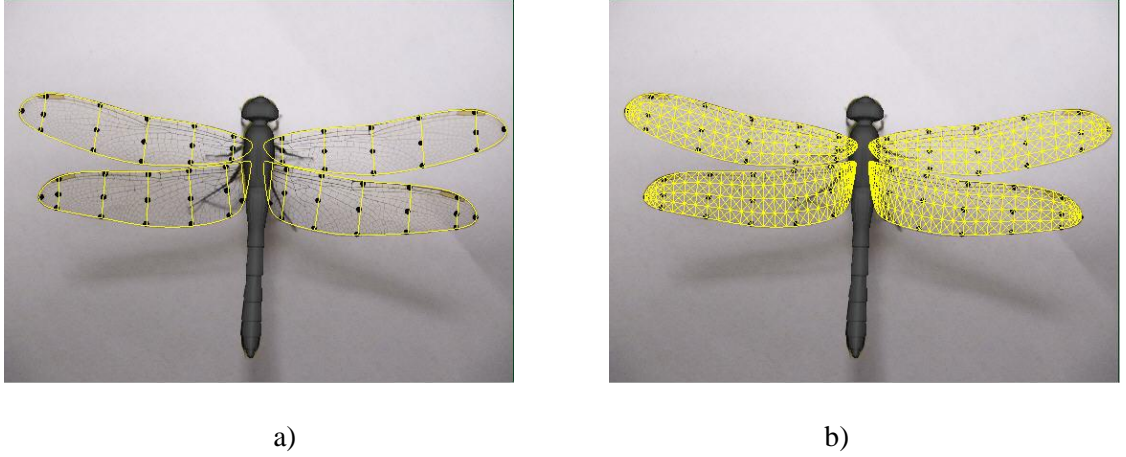


Figure 2 Reconstructed model built by Autodesk MAYA. a) Initial model by tracking markers on wings. b) Fine meshed model to create more points.

Since the whole motion of takeoff maneuver in a video is to be studied, we may take advantage of the key points on the NURBS surfaces to animate the position of markers on the wings in every frame until a significant motion is reconstructed as an animation. Then we mesh the wing models finely to produce enough points for all the information about real wings' surfaces. Triangulating the original rectangular surface grids is used to compute the data from reconstruction directly onto the in-house solver (introduced in the section on DNS). The model containing the resultant fine meshes is shown as Figure 2 b). One example of using reconstructed model into a frame of images

shot by photogrammetry system is displayed in Figure 3, where the reconstructed model is fully matched with the image. In addition, the dragonfly's body is assumed to be rigid and is not important compared to the contribution by its wings. During reconstruction, the wings' deformation during clap involves twist but not camber.

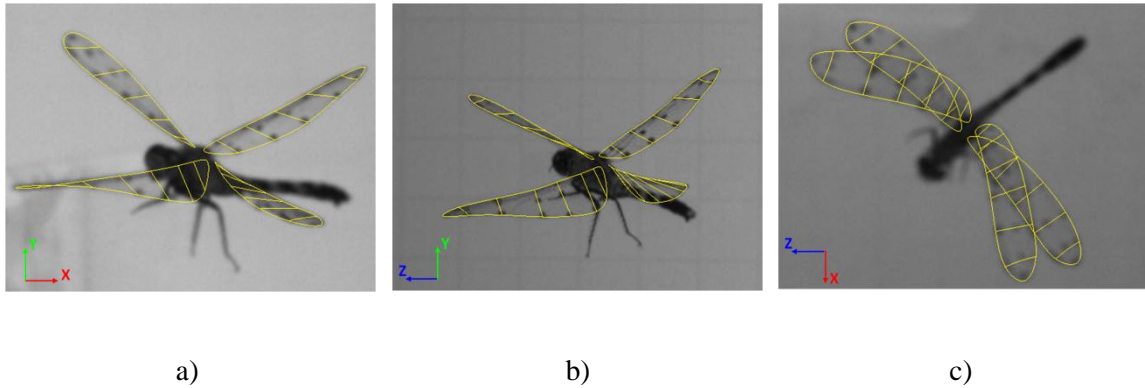


Figure 3 Three dimensional surface reconstruction. a) Front view which coordinate is with respect to X and Y axes. b) Side view with respect to Y and Z axes. c) Top view with respect to X and Z axes.

## 2: Design of Wing-Damage Experiment

### 2.1: Species of Dragonfly and Environment in laboratory

In the experiment of wing damage, 15 dragonflies which are *the Eastern Pondhawk (Erythemis simpliciolis)* are filmed in high-speed photogrammetry laboratory to study free flight takeoff maneuver. Those dragonflies were caught between 10 July and 31 August 2011 near the pond of Nutter Center in Wright State University. They were stored temporarily in a big plastic container during capture and then were moved into indoor laboratory maintained at a temperature of 20 °C. To film the flying motion of

dragonflies without any interference, the door and the air conditioner were closed to reduce the effect of air flow. Also, the temperature was increased to approximate 26 °C to keep the dragonflies active. However, owing to the rapid shutter speed, a large amount of light is required during image shooting. This light adds more and more heat as time goes by, and the temperature of the shooting area is affected and increased obviously. The high temperature could reduce the activity of dragonflies. Also, the bright light and the reflection from the white background (shown in Figure 1) make dragonflies get wrong information about environment, and so sometimes the dragonflies during filming crash to the white board. Thus, controlling the indoor temperature and the light impact is very important for dragonflies' free flight. In addition, all the dragonflies were tested within 5 hours of capture to ensure their activeness.

## 2.2: Implementation of Experiment

For every single dragonfly, its wings have to be marked by a set of dots before filming so that it is possible to track wing clap motion during flight by using reconstruction technology (explained in reconstruction part). The weight from the ink of those dots could be neglected since a fine permanent marker is selected. To track more accurately and conveniently in the reconstruction procedure, while also ensuring negligible mass of ink added, the amount of marker points must be limited and should also be able to fully describe the shape and the deformation of dragonflies' forewings and hindwings. Therefore, the distribution of markers adopted is shown as Figure 4 a). The profile of wings could be fully described by the dots on their edges, and the dots on the

middle span aid in tracking of the deformation during free flight. Also, the markers are distributed evenly both on the span-wise and chord-wise directions.

After a dragonfly is marked, it will be filmed at least three times so that the motion is general and convenient to compare. The images could be seen as the normal flight of the individual with intact wings. Then the individual's single wing is damaged, and the flying motion should be filmed at least three times; finally, the symmetric wing is supposed to be cut, and similarly the flight of the individual with damage on double wings should be shot three times.

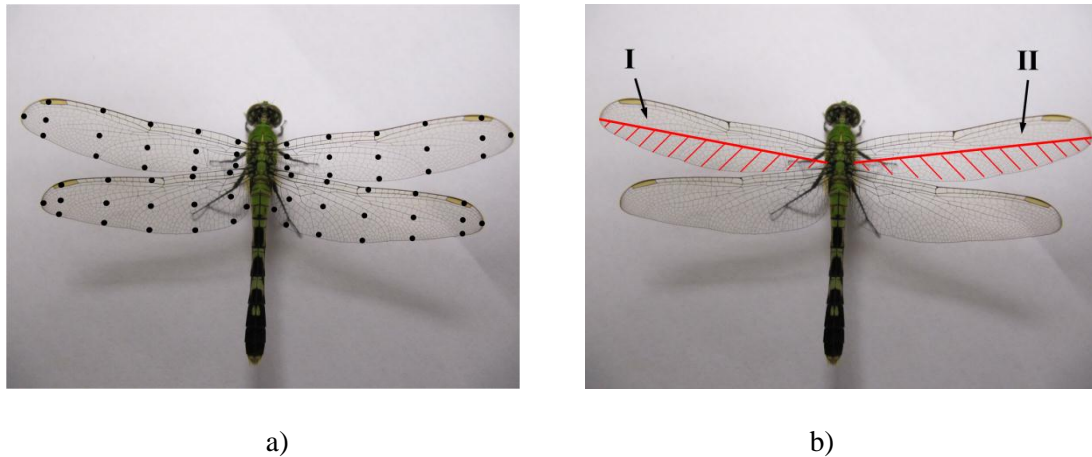


Figure 4 One studied dragonfly with artificial markers and the damaged area on the forewings. a) Markers on the four wings. b) Damaged area on the forewings.

The hatched parts I and II are the loss area.

The main purposes of designing wing-damage experiments are to know the role of forewing in dragonfly maneuverability and the effect of wing area loss on performance of free flight. Based on the characteristic of dragonfly wings in flight and the purposes of

the experiment mentioned above, the damaged area is determined along the span of wings, and the damaged area is 40% of an entire forewing, as shown as Figure 4 b). The red hatched part is supposed to be cut off, and the damaged area should be symmetric if both wings need to be cut. That is, for example, after the flight of a dragonfly with left forewing damage (Area I in Figure 4 b)) is filmed, the right forewing is supposed to be cut, and the cutoff area should be coincident with that of the left forewing (Area II in Figure 4 b)).

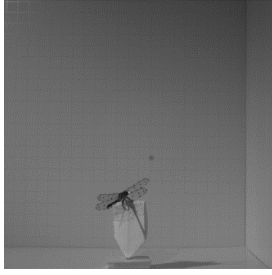
After the experiments were finished, three sets of images from one of 15 dragonflies are selected to investigate since they have similar free flying motion but with different damaged situations. Table 1 shows the free flying motion in the three cases (IW, OFD, and DFD).

	Flying motion
<u>I</u> ntact <u>W</u> ings (IW)	Takeoff with left turn (90 °)
<u>O</u> ne-sided <u>F</u> orewing <u>D</u> amage (OFD)	Takeoff with left turn (90 °)
<u>D</u> ouble-side <u>F</u> orewing <u>D</u> amage (DFD)	Takeoff with right turn (180 °)

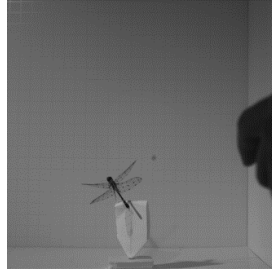
Table 1 Flying motion of the dragonfly in the three cases

As shown in Table 1, the motion in each case is takeoff maneuver. In the IW case, the dragonfly that had intact wings turned to left almost 90 ° when it took off, and there was a slight rise in vertical direction within 0.223s. Then the left forewing was cut off 40% along span in the OFD case, and that dragonfly went through 180 ° in the similar direction

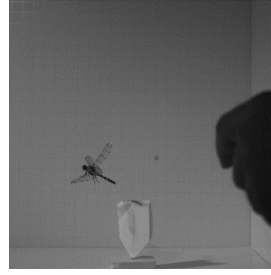
as the IW case when it took off. However, it flew down in vertical direction during turning. After the turning motion was finished, it kept climbing up and flew through a very long distance in vertical direction within 0.290s. The DFD case presented that the same dragonfly as IW and OFD, where both forewings were damaged, made takeoff with  $180^\circ$  right turning, but the vertical traveling distance was negative if a rise is defined as positive direction. All the cases mentioned above are shown in Figure 5, the pictures are randomly chosen to illustrate the entire flying motion.



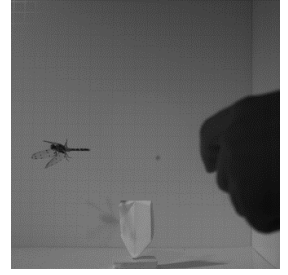
a)  $t_1 = 0.028s$



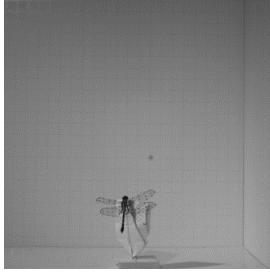
$t_2 = 0.149s$



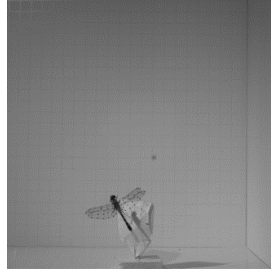
$t_3 = 0.201s$



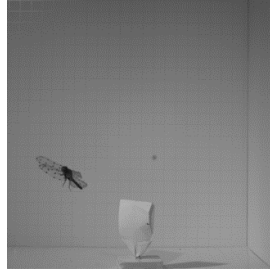
$t_4 = 0.251s$



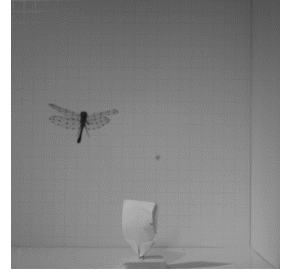
b)  $t_1 = 0.058s$



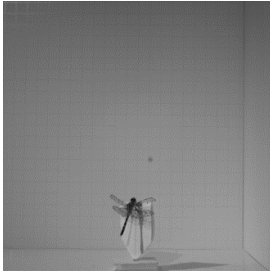
$t_2 = 0.11s$



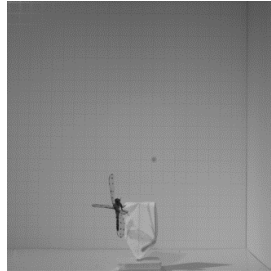
$t_3 = 0.267s$



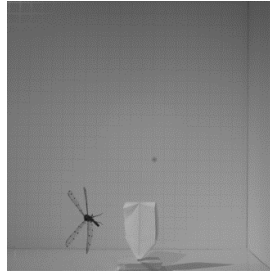
$t_4 = 0.348s$



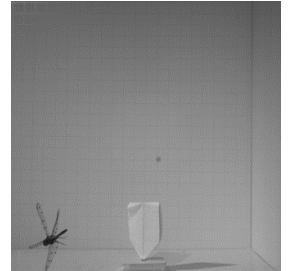
c)  $t_1 = 0.005s$



$t_2 = 0.085s$



$t_3 = 0.130s$



$t_4 = 0.168s$

Figure 5 Motion in different time of the three cases filmed by 3D High speed photogrammetry system. a) IW, b) OFD, c) DFD.

### 3: Coordinate Transformation

In this thesis, the basic data of dragonflies' free flight which are obtained from Autodesk MAYA consists of the displacement of nodes on the model's body and wings and is based on the coordinate shown in Figure 6. To get the instantaneous displacement related with the original position of dragonflies, the origin 'O' of the coordinate could be simply transformed to the center of dragonflies' body mass. The displacement obtained is the position with respect to the starting location where dragonflies fly.

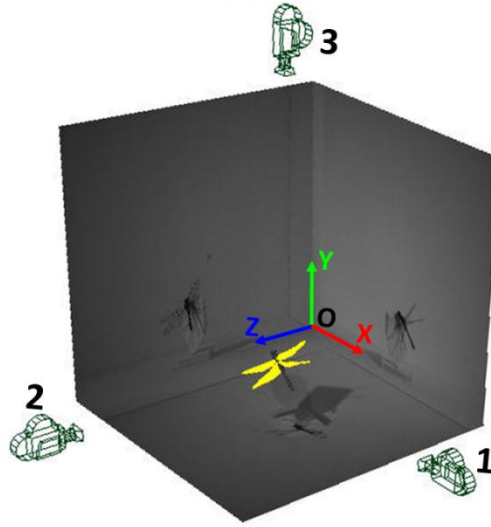


Figure 6 Global Cartesian coordinate in reconstruction system. The origin 'O' is coincident with the intersection point of XZ, XY, and YZ plane. XZ plane is corresponding to the top-view images from Camera 3. XY plane is with respect to the front-view images from Camera 2, and YZ plane is corresponding to the

side-view images from Camera 1. The position of three cameras mimics the high-speed photogrammetry system in laboratory.

In order to compute wing kinematics, the global coordinate above should be transformed on dragonflies' bodies by using Euler transformation. The transformed coordinate with respect to body is called local coordinate system and is shown in Figure 7.

Since the dragonflies' wings do asymmetric motion when they are turning, different wings should have different stroke planes. Also, the trajectory of one wing in different strokes is different, so the mean stroke plane is supposed to be changed when the wing moves to the next stroke. Owing to the complexity of wing motion, the mean stroke plane is defined as a least square plane with respect to the tip path within one stroke. For example, Figure 7 shows the left forewing's mean stroke plane in one stroke.

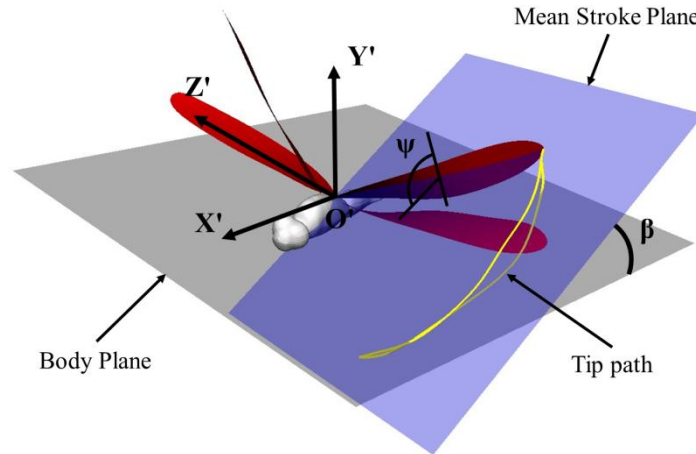


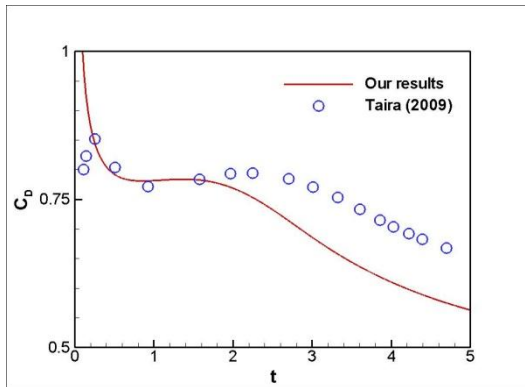
Figure 7 Local coordinate system when investigating wing kinematics. The origin  $O'$  is on the wing root.  $X'$  axis is parallel to the dragonfly's body axis which points from tail to head.  $Y'$  axis is normal to the body axis and points from body's bottom to top.  $Z'$  axis is perpendicular to  $X'$  and  $Y'$  axis and points to right of the dragonfly's body. Body plane is perpendicular to the Plane  $X'Y'$ . The blue



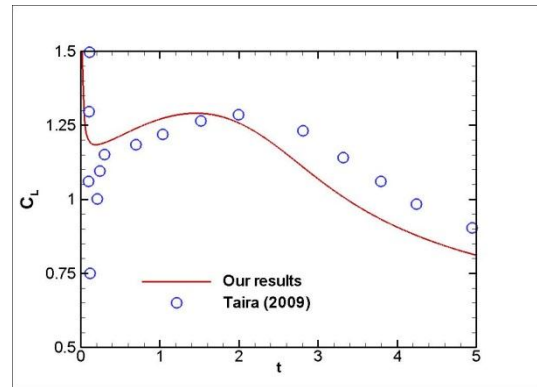
plane which passes through the left forewing (LF) is the mean stroke plane of LF in terms of one stroke itself. Yellow line is the tip path within the one stroke.  $\theta$  is the pitching angle of wings, and  $\beta$  is stroke plane angle with respect to the body plane.

#### 4: Direct Numerical Simulation method (DNS)

The aerodynamic performance including lift and vortex generation is solved by a validated in-house CFD solver (Dong, 2006; Mittal et al., 2008). This solver that is also called PiCar 3D solver uses non-uniform Cartesian grids and can simulate incompressible viscous flow when the region of Reynolds number is from  $O(10^1)$  to  $O(10^3)$  which is suitable for insects' flight. Also, ghost-cell methodology and a sharp interface immersed boundary method are introduced to deal with complicated three-dimensional body surfaces which are composed of unstructured tri-angular elements. Figure 8 shows the validation for the solver. The case for validation is set as three dimensional flows over a semi-circle plate with aspect-ratio  $AR = \frac{8}{\pi}$ , angle of attack  $\alpha=30^\circ$ , and  $Re=300$  (Taira et al., 2009).



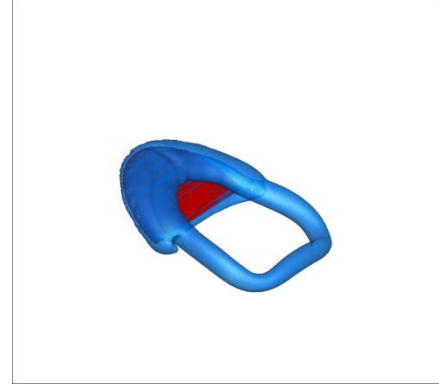
a)



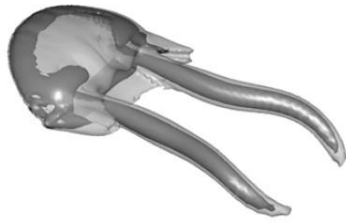
b)



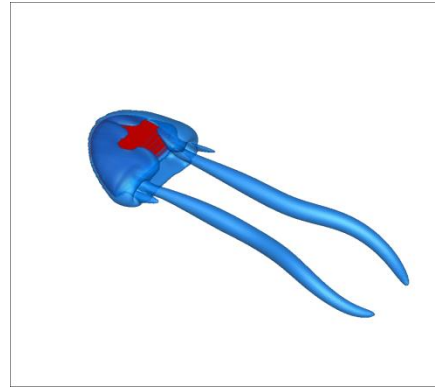
c)



d)



e)



f)

Figure 8 Validation case. a) and b) show the comparison of lift and drag coefficient from PiCar 3D solver and Taria 2009. c) and d) present wake vorticity behind the plate at  $t=1.5$ . e) and f) presents wake structure behind the plate at  $t=5.0$ . c) and e) are the results from Taria 2009, and d) and f) are computed by PiCar 3D solver used in this thesis.

### III. RESUTLS AND DISCUSSIONS

#### 1: Morphological parameters

The dragonfly's morphological parameters including mass, mid-chord length of forewings and hindwings, and mid-span length of forewings and hindwings were measured before the experiments, as shown in Table 2. The left wings and right wings are assumed to be symmetric and identical to each other.

		Data
Mass (g)		0.062
Forewing (mm)	Span Length	30.2
	Chord Length	8.4
Hind Wing (mm)	Span Length	29.4
	Chord Length	8.9

Table 2 Morphological parameters of the individual

The dragonfly's mass in the OFD and DFD cases was measured respectively. Results showed that the mass of wing area removal is less than 1% of the body mass for the two cases, so the mass of cut-off wing area could be neglected and will not influence the following results. In addition, note that this dragonfly is the lightest of the 15 dragonflies used, but the size of the body and the magnitude of wings are similar to the other dragonflies captured, so the result should be general.

## 2: Mean Wing beat frequency

For all the cases selected above, we recorded the whole flight from the takeoff position until the dragonfly moved out of the filming domain. However, generally the takeoff maneuver could be finished within two or three wing strokes. Thus, a window of 0.08s was chosen in each of the cases for analysis. The frequency of different wings in different cases is obtained by both measurement and computation. Since free flight of takeoff maneuver is complicated, even two forewings of a dragonfly have different frequencies. After dealing with raw data directly output from MAYA, we observed that 2 complete strokes for all four wings are involved in the IW and OFD case; 2 strokes for forewings and 2.5 strokes for hindwings are contained in the DFD cases. Table 3 lists the average frequency of the four wings respectively.

Case	Left Forewing (Hz)	Left Hindwing (Hz)	Right Forewing (Hz)	Right Hindwing (Hz)
IW	26.6	27.7	27.5	25.8
OFD	27.9	27.8	26.7	28.2
DFD	27.5	29.1	27.6	30.1

Table 3 Mean wing beating frequencies of four wings in the three cases

## 3: Displacement of the dragonfly's body

The variation of the displacement during the whole flight is a basic parameter to understand free flying process of takeoff maneuver. The qualitative data of the displacement for every single point on the body can be output from MAYA file, which is

based on the global Cartesian coordinate system (shown in Figure 6) and is the raw data for the subsequent analysis.

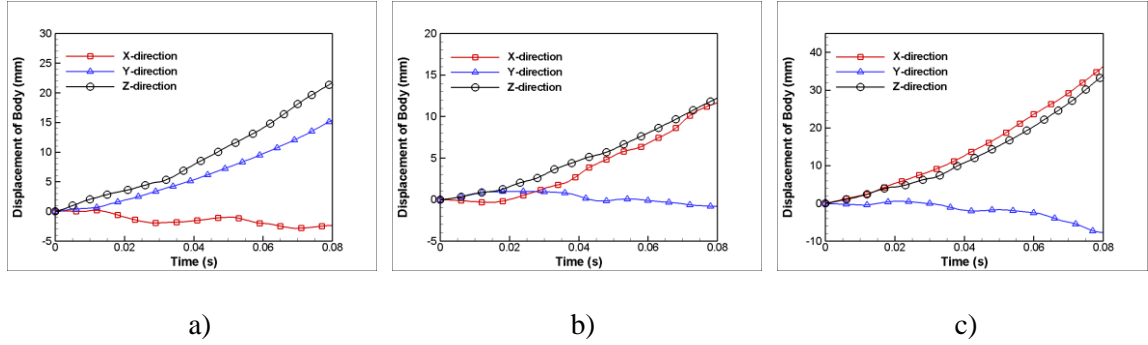


Figure 9 Time history of displacement in three directions. a) IW. b) OFD. c)

DFD. The red line with square symbols stands for x-direction displacement, the blue line with delta symbols stands for y-direction displacement, and the black line with circle symbols stands for z-direction displacement.

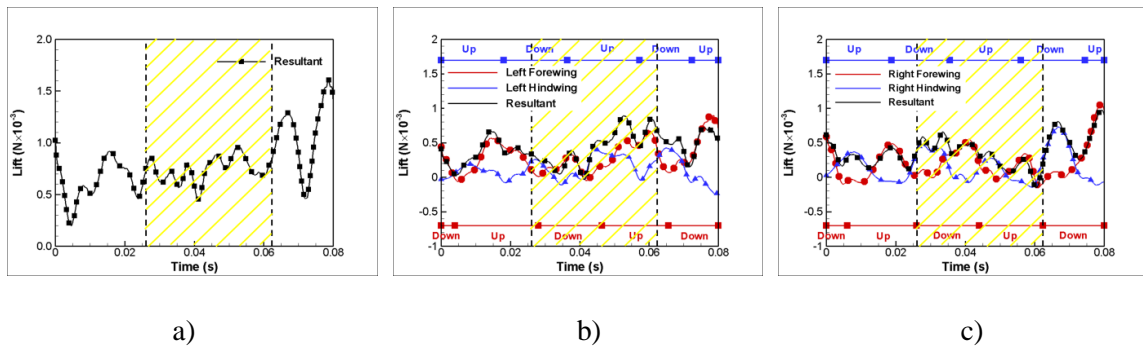
Figure 9 displays the instantaneous displacement of center of mass in the three cases. a) illustrates the displacement in the IW case. The x-direction displacement decreases, that is, the dragonfly is flying close to the YZ plane shown in Figure 9; the increasing displacements in y- and z-direction shows that the individual is rising and flying away from the XY plane. Figure 9 b) displays that the dragonfly in the case OFD is flying away from the XY and YZ plane but flying down slightly since the y-direction displacement is decreasing. 9 c) shows that in the case of DFD the dragonfly flies twice distance in x and z direction but has more decrease on vertical direction compared to a) and b). Consequently, comparing all the three cases, only the IW case performs the

increase on vertical displacement, while the other cases illustrate drops in the y direction when the dragonfly is doing a takeoff with turning motion.

#### 4: Lift performance

##### 4.1: Resultant Lift

In terms of the three cases, the lift performance has to be different due to the difference of wing area loss and the difference of turning directions. From this section onwards, the left wings and the right wings are defined as inner wings and outer wings respectively if the dragonfly flies to left. Correspondingly, if the dragonfly turns to right, its left wings and right wings are defined as outer wings and inner wings respectively. Figure 10 shows the lift forces generated by four wings during 0.08s, which includes more than two complete strokes of forewings and hindwings for the IW, OFD, and DFD cases.



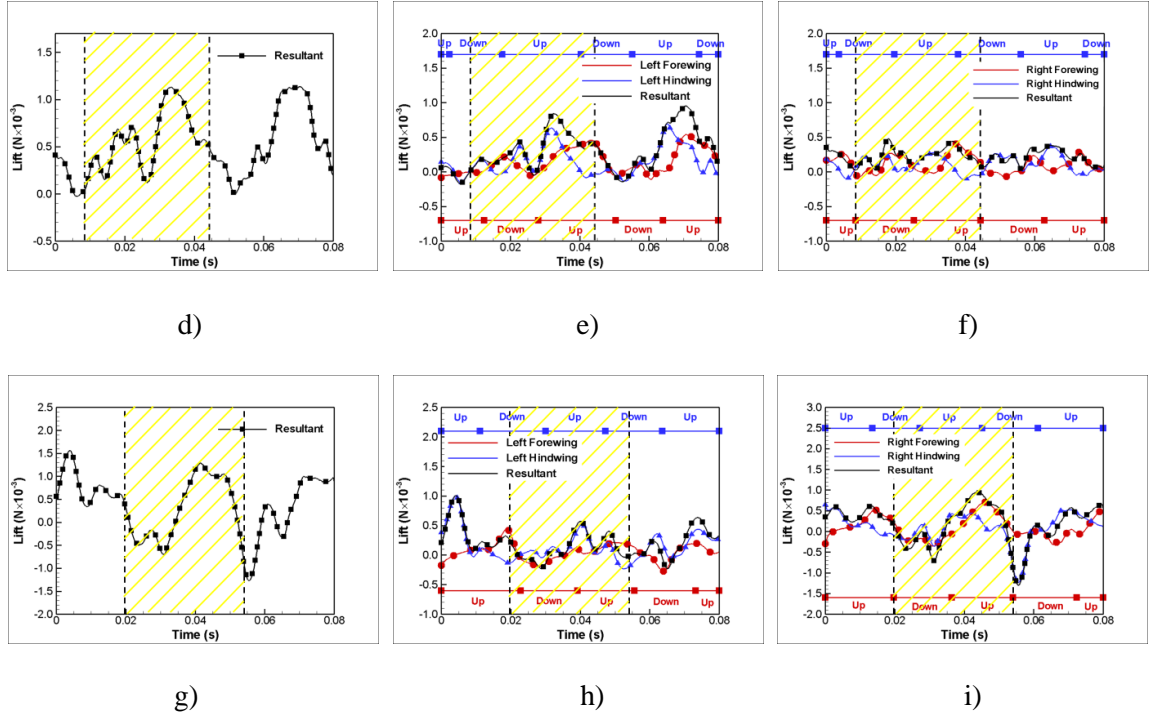


Figure 10 Instantaneous lift generated by the individual's four wings during 0.08s.

a), b), c) IW, d), e), f) OFD, g), h), i) DFD. a), d), and g) in the first column show the resultant lift generated by four wings. b), e), and h) illustrate the lift generated by left wings, and c), f), and i) display the lift generated by right wings. In figures at the second and last column the red line stands for the instantaneous lift generated by forewings, the blue line stands for the lift generated by hindwings, and the black line stands for the resultant lift of forewing and hindwing on the same side. Up and Down represent upstrokes and downstrokes. Due to the turning direction of the three cases, b), e) and i) presents the lift generated by the inner wings, c), f), and h) presents the lift generated by the outer wings.

Figure 10 a) shows that, most of the time the instantaneous resultant lift is greater than the dragonfly's weight, and it keeps increasing. At the end of the studied period the resultant lift reaches to  $1.5 \times 10^{-3}$  N. It is an accelerated takeoff motion. However, in d),

the resultant lift appears to have a sharp drop and rise due to the left forewing damage. The maximum value at the two biggest peaks only can approach  $1.1 \times 10^{-3}$  N. The minimum resultant lift is still larger than zero, but most of the time, the lift is less than the force due to gravity. g) illustrates that the resultant lift in the DFD case appears to have a periodic decline and rise, and the trend of the resultant lift keeps decreasing during the studied period due to the effect of 40% wing area loss on each forewing; The maxima in each period of this oscillation drops from  $1.5 \times 10^{-3}$  N to  $1.3 \times 10^{-3}$  N, and then to  $1.0 \times 10^{-3}$  N. In more than 30% of the total period, the resultant lift is negative, that is, the resultant plays a resistant role in takeoff motion. The minimum value reaches to even  $-1.2 \times 10^{-3}$  N.

In Figure 10 b) and c), both inner wings and outer wings generate large lift during the whole period of the dragonfly left turn. The lift forces produced by the forewing and hindwing at the same side complement each other well since the lift forces produced by forewings is increased when the lift produced by hindwings is decreased. However, in e) and f) the lift generated by the inner wings fluctuates a lot compared to the outer wings in the OFD case, and the maximum lift is obtained from the left hindwing. In addition, comparing c) and f), we see that f) has a smaller magnitude of lift forces on the outer wings. For the DFD case (Figure 10 h) and i)), the inner wings generate more lift than the outer wings, which is similar to the case of OFD. However, the lift on the right hindwing in the DFD case shows a sharp drop in the following downstroke of the selected stroke. The two damaged forewings are able to generate a lift around zero (especially the outer forewing). In conclusion, the lift distribution on the inner and outer wings in the IW case is similar; whereas, after a forewing is damaged, the lift generation on the inner and outer wings will be changed based on its turning direction. For example, even if the left



forewing is cut off 40% in the OFD case, most of the time the lift generated by left wings (inner wings) is bigger than right wings (right wings) since the dragonfly is turning left. The DFD case also illustrates the same characteristics.

#### 4.2: Lift on individual wings

In order to examine detailed variation of lift forces on each wing, one stroke of the right forewing (starting from downstroke to upstroke) is chosen in each case. The stroke of hindwings is not considered since their frequencies change after the two forewings lose 40% of wing area (in Table 3). The time regions for the three cases are depicted as the yellow hatched domain in Figure 10. In order to study the difference of distribution of lift performance between the IW case and wing damage cases (OFD and DFD), the mean lift force on each wing and its percentage of mean total lift could be utilized for a comparison. Table 4, Table 5, and Table 6 display the mean value of total lift force, and lift force on each wing in the selected stroke in the three cases respectively. In addition, Table 7 shows the mean lift information in the following downstroke for the three cases.

	Downstroke		Upstroke	
	Mean Lift ( $N \times 10^{-3}$ )	Percentage (%)	Mean Lift ( $N \times 10^{-3}$ )	Percentage (%)
Total Lift	0.7	--	0.8	--
Left Forewing	0.1	14	0.4	50
Left Hindwing	0.1	14	0.2	25
Right Forewing	0.3	43	0.1	12.5

Right Hindwing	0.2	29	0.1	12.5
----------------	-----	----	-----	------

Table 4 Mean lift on the four wings and the percentage of the mean lift on each wing for the downstroke and upstroke in the IW case.

	Downstroke		Upstroke	
	Mean Lift ( $N \times 10^{-3}$ )	Percentage (%)	Mean Lift ( $N \times 10^{-3}$ )	Percentage (%)
Total Lift	0.4	--	0.7	--
Left Forewing	0.1	25	0.2	29
Left Hindwing	0.1	25	0.2	29
Right Forewing	0.1	25	0.2	29
Right Hindwing	0.1	25	0.1	13

Table 5 Mean lift on the four wings and the percentage of the mean lift on each wing for the downstroke and upstroke in the OFD case.

	Downstroke		Upstroke	
	Mean Lift ( $N \times 10^{-3}$ )	Percentage (%)	Mean Lift ( $N \times 10^{-3}$ )	Percentage (%)
Total Lift	-0.3	--	0.8	--
Left Forewing	-0.1	--	0.1	12.5
Left Hindwing	0	--	0.1	12.5
Right Forewing	-0.2	--	0.4	50
Right Hindwing	0	--	0.2	25

Table 6 Mean lift on the four wings and the percentage of the mean lift on each wing for the downstroke and upstroke in the DFD case.

	IW		OFD		DFD	
	Mean Lift ( $N \times 10^{-3}$ )	Percentage (%)	Mean Lift ( $N \times 10^{-3}$ )	Percentage (%)	Mean Lift ( $N \times 10^{-3}$ )	Percentage (%)
Total Lift	1.1	--	0.3	--	0.1	--
Left Forewing	0.4	36	0.1	33.3	0	--
Left Hindwing	0.1	10	0	0	0.1	--
Right Forewing	0.3	27	0.1	33.3	-0.1	--
Right Hindwing	0.3	27	0.1	33.3	0.1	--

Table 7 Mean lift on the four wings and the percentage of the mean lift on each wing for the following downstroke of the one stroke studied in the IW, OFD, and DFD cases.

Firstly, the effect of forewing damage on lift performance could be seen from the variation of mean total lift forces. In the IW case, the mean value of total lift during the three half strokes keeps increasing and is always greater than the dragonfly's weight (0.6g). In contrast, the mean total lift in the case of OFD and DFD in the downstrokes (Table 5, Table 6 and Table 7) is much less than the IW case. In the DFD case the total lift force in the downstroke is negative. In the upstroke the total lift of the two damaged wing cases is close to the IW case. Consequently, the dragonfly with damaged forewings cannot produce lift efficiently, that is, wing area removal on forewings will mainly impact the lift performance during downstroke. Also, the flight of takeoff motion with two-sided forewing damage will become unstable.

In addition, during the motion of takeoff maneuver, the lift generation no longer satisfies the normal force generation pattern in which one observes that the lift is always produced more in the downstroke than the upstroke. For example, in Table 4 the total lift in the upstroke is larger than the downstroke since the dragonfly has to keep increasing lift to finish a fast takeoff motion (The following downstroke produces more lift force than the upstroke shown in Table 7). However, in the OFD and DFD cases, the lift in the downstroke cannot be maintained as in the IW case anymore, and the upstroke has to be dominant to produce lift forces in takeoff motion.

Secondly, since the number of the forewings damaged in each case is different, the lift performance on each wing is also different. Compared to the IW case, the OFD case (shown in Table 5) shows that in the downstroke, mean lift generated by the inner wings is not reduced although 40% of left forewing area is lost. But the outer wings produce less lift. Also, the percentage of the lift generated by each wings in downstroke is recorded. Comparing the third column in Table 4 and Table 5, although the left forewing generated the same vertical force after cutting as when intact, its contribution to the total lift is more important since the percentage of total lift increases from 14% to 25%. Also, the left hindwing becomes more important for providing lift in the downstroke after the left forewing is damaged, and its value reaches to about 25% of total lift. Conversely, the vertical forces from the right forewing and the right hindwing drop by 18% and 4% respectively due to effect of the left forewing damage. On the other hand, in the DFD case, the mean lift produced by the left and right hindwings is approximately zero. The two damaged forewings provide negative lift forces which have an opposite direction to the lift, especially the right forewing generates a large resistant force when it

was damaged. This may be the reason why the flight of the dragonfly in the case DFD is unstable.

Finally, although the mean lift force generated by the four wings is not influenced by the damage during upstroke, there is a redistribution of lift on the four wings. Comparing the vertical forces separately in the upstroke for the IW and OFD cases, the lift force from the inner wings totally drops by nearly 50% after the left forewing is damaged, while the mean lift produced by the outer wings is increased especially by the right forewing. Consequently, all the loss of total lift in the OFD case comes from the left forewing since the total lift drops by  $0.1 \times 10^{-3}$  N, while the lift from left forewing decreases by  $0.2 \times 10^{-3}$  N. Also, according to the values of percentage shown in the last column of Table 4 and Table 5, even if the lift produced by the inner wings decrease due to wing damage, the left forewing still plays the most important role in producing lift (as in the case of IW). In contrast, the right hindwing (the outer wing) provides the least vertical force during upstroke in both the IW and OFD cases. The magnitude of lift produced by the right forewing in the OFD case is twice the magnitude of the IW case. In the DFD case, the mean lift performance on each wing is the same as the IW case during upstroke. 50% of total lift comes from the damaged right forewing (the inner wing), and the right hindwing also generates a large amount of lift force. The outer wings only provide 25% of total lift force, which are less than the right forewing.

On the other hand, the instantaneous lift and the resultant lift of the inner wings and outer wings in one stroke for the three cases are examined, as shown in Figure 11. First of all, Figure 11 a) shows the variation of the vertical force on the inner wings in the case of IW. The lift from the left forewing is nearly close to zero at the beginning of the

downstroke, and after five small peaks approaches a value of  $0.4 \times 10^{-3}$  N, and the maximum value,  $0.67 \times 10^{-3}$  N, displays at 0.034s at the end of the upstroke. However, the maximum value of resultant lift,  $0.89 \times 10^{-3}$  N, for the inner wings is at 0.027s. The lift from left hindwing starts from  $0.22 \times 10^{-3}$  N and ends at  $0.25 \times 10^{-3}$  N. The maximum value  $0.38 \times 10^{-3}$  N appears in the supination. During the whole stroke, the trend of resultant lift of the inner wings follows that of left forewing, that is, the left forewing during downstroke is dominant for generating lift forces. Figure 11 b) shows the lift variation of the outer wings in the IW case. The force from the right forewing starts at nearly zero and goes through three peaks then ends at zero. The maximum value  $0.56 \times 10^{-3}$  N happens at 0.015s. The lift produced by the right hindwing begins at  $0.35 \times 10^{-3}$  N and has a largest value at the beginning of the downstroke ( $0.47 \times 10^{-3}$  N). The second peak is in the supination of the right forewing, and its magnitude is  $0.28 \times 10^{-3}$  N. At the end of the upstroke, there is a sharp rise on the lift produced by the right hindwing, and the value is changed to  $0.26 \times 10^{-3}$  N at the end of the whole stroke. The trend of resultant lift of the outer wings also follows the corresponding forewing, and one obvious peak with a value of  $0.67 \times 10^{-3}$  N happens in the downstroke. The maximum value of the lift produced by the right wings is less than the left wings. However, the maximum lift generated by the inner wings happens in the upstroke, while the maximum value of the outer wings appears in the downstroke.

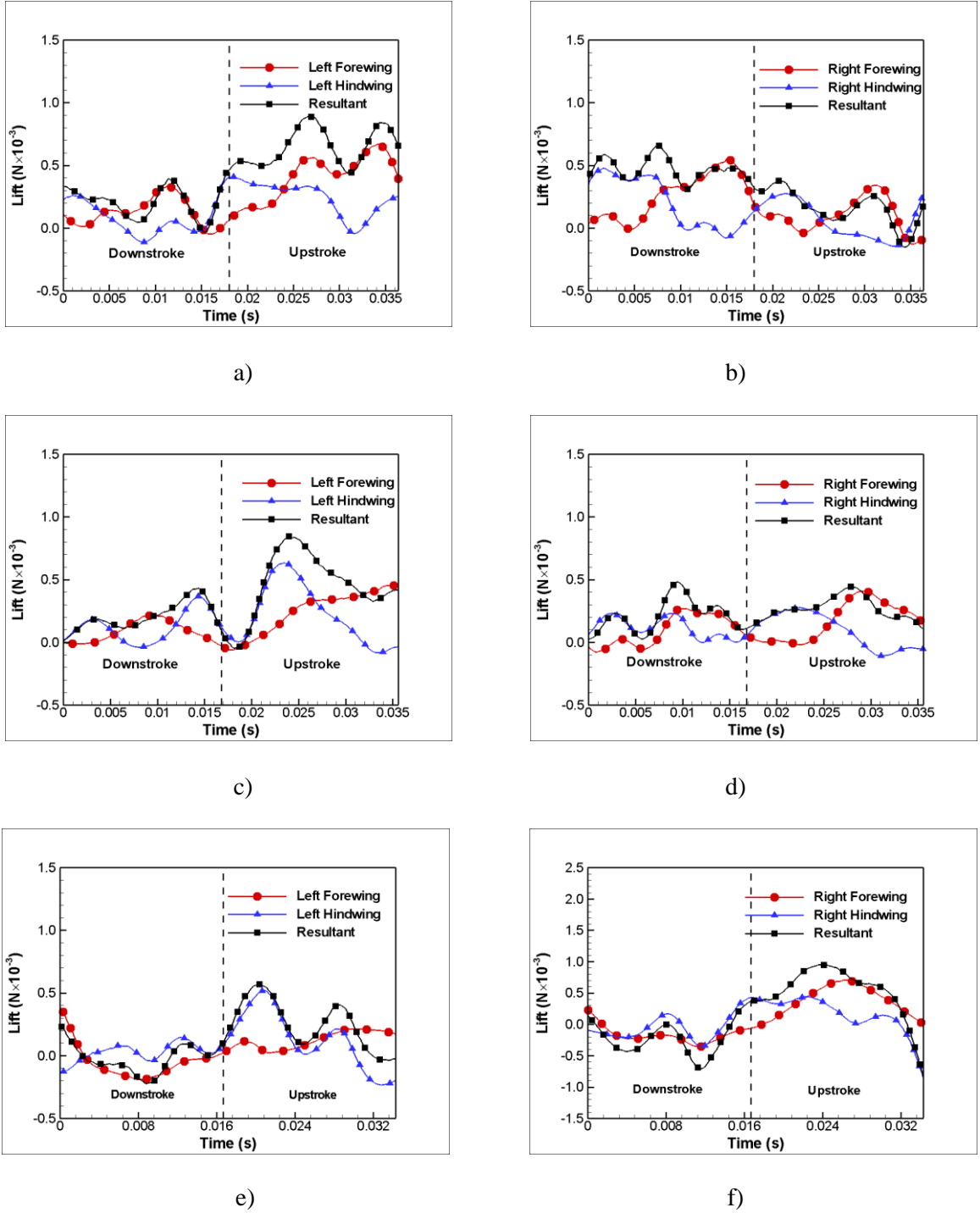


Figure 11 Lift for four wings versus time in one completed stroke. a) and b) IW.

a) Lift for the inner wings, b) Lift for the outer wings. c) and d) OFD. c) Lift for the inner wings, d) Lift for the outer wings. e) and f) DFD. e) Lift for the outer wings, f) Lift for the inner wings. The red line with cycle symbols stands for

forewings; the blue line with delta symbols stands for hindwings; the black line with square symbols stands for resultant of the inner wings or outer wings.

Figure 11c) and Figure 11d) show the time history of the lift forces on individual wings in the OFD case. In Figure 11 c), the lift generated by the left forewing is changing steadily due to the 40% loss of the wing area, but the blue line which presents the vertical force on the left hindwing varies erratically. There are three peaks on the blue line within the selected domain which are larger than the red line. The values are  $0.18 \times 10^{-3}$  N,  $0.37 \times 10^{-3}$  N, and  $0.63 \times 10^{-3}$  N respectively. Also, the lift on the left hindwing starts from zero and ends at  $-0.04 \times 10^{-3}$  N. The minimum value  $-0.08 \times 10^{-3}$  N appears at the end of the upstroke when the left forewing provides the maximum value of lift,  $0.45 \times 10^{-3}$  N. The trend of the resultant force of the inner wings follows the left hindwing, so the left hindwing is dominant to produce lift force which is different from the IW case. In Figure 11 d), the lift produced by the outer wings varies slightly. The vertical lift on the right forewing has a maximum value  $0.41 \times 10^{-3}$  N at 0.029s, but the resultant force does not reach the largest magnitude at that time. The minimum of the right forewing's lift is close to zero. For the lift generated by the right hindwing, the maximum value  $0.27 \times 10^{-3}$  N appears at the beginning of the upstroke of the right forewing, and the minimum,  $-0.1 \times 10^{-3}$  N, is shown at the end of the upstroke. The resultant force has the minimum  $0.02 \times 10^{-3}$  N at 0.005s and the maximum  $0.48 \times 10^{-3}$  N at 0.009s. Both of these values are present in the downstroke. In the upstroke, the second peak happens in 0.028s with a value of  $0.44 \times 10^{-3}$  N. In the whole stroke, the individual lift produced by the right forewing and right hindwing varies within a limited range.



The lift force on each wing in the DFD case is displayed in Figure 11 e) and f). Firstly, for the left forewing (the outer wing) which has lost 40% of the wing area in Figure 11 e), the lift generated starts from  $0.4 \times 10^{-3}$  N and end at  $0.2 \times 10^{-3}$  N; it has the minimum value of  $-0.2 \times 10^{-3}$  N in the downstroke and has a maximum value of  $0.2 \times 10^{-3}$  N in the upstroke; it performs as resistance during downstroke, where it is always negative, but helps rising during upstroke in which all instantaneous values are above zero. Secondly, the lift on the left hindwing (the outer wing) starts and ends at values below zero respectively; after two small peaks it approaches the maximum,  $0.5 \times 10^{-3}$  N, at the beginning of the upstroke of the right forewing; the minimum value is  $-0.2 \times 10^{-3}$  N. The trend of the resultant force from the outer wings follows the variation of the left hindwing, that is, the left hindwing performs most lift to help the dragonfly turn right. The maximum value of the resultant force on the outer wings is  $0.6 \times 10^{-3}$  N in which the left hindwing accounts for 87%. The second obvious peak appeared at 0.028s is  $0.4 \times 10^{-3}$  N, and 53% is from the left hindwing. Thirdly, Figure 11 f) shows the time history of lift generated by the inner wings. The lift on the right forewing changes slightly, begins to increase at the end of the downstroke, and reaches to  $0.7 \times 10^{-3}$  N in the middle of the upstroke, then decreases sharply to zero. The lift produced by the right hindwing displays a peak value,  $0.2 \times 10^{-3}$  N, at 0.007s, and then it drops suddenly to  $-0.4 \times 10^{-3}$  N. After that it increases again and reaches to  $0.4 \times 10^{-3}$  N at the reverse of the right forewing, the maximum value during the whole stroke, and the minimum is  $-1.2 \times 10^{-3}$  N at the end of the upstroke. The resultant force on the inner wings reaches  $0.95 \times 10^{-3}$  N at 0.022s after a few fluctuations; the minimum value  $-1.3 \times 10^{-3}$  N is seen at the same time as the

minimum value of the right hindwing, and the lift on the right hindwing accounts for 95% of the resultant.

In conclusion, the maximum value of lift is always displayed on the left forewing in the IW case (Figure 11 a)) compared to the left hindwing, while the left hindwing in the OFD case (Figure 11 c)) always generates larger lift than the left forewing. In the other words, when the left forewing loses 40% of wing area, the lift produced will be affected immediately. Therefore, the left hindwing becomes more important on supplying lift. For b) and d), the resultant force of the outer wings in the IW case during downstroke is larger than the upstroke. However, due to the effect of the left forewing damage, the outer wings provide less lift in the whole stroke in d).

Also, comparing Figure 11 c) and f) which stand for the instantaneous lift generated by the inner wings, the similarity is that the resultant lift is dependent on the hindwing. The difference is that the lift on the hindwing in the DFD case has a smaller peak value but a larger minimum value than the OFD case. Figure 11 d) and e) shows a similar trend on the lift performance of the outer wings. The left hindwing in the DFD case gives a very large value during upstroke comparing with the OFD case.

The lift validations for the three cases in the time region are displayed in Table 8. As shown in Table 1, the dragonfly's mass is 0.062g ( $mg=0.6 \times 10^{-3}N$ ). The total lift production in the stroke could be validated by comparing the acceleration from kinematics and from aerodynamics. In Table 8,  $a_k$  is obtained by  $\frac{\Delta v}{\Delta t}$ .  $\Delta v$  is the velocity difference within  $\Delta t$ , which is the time of the selected stroke. In the IW case,  $\Delta v = 0.23m/s$  within 0.036s; In the OFD case,  $\Delta v = -0.05m/s$  in 0.0356s; In the DFD case,  $\Delta v = -0.14m/s$  in 0.034s.

	IW	OFD	DFD
Mean Lift ( $\text{N} \times 10^{-3}$ )	0.7	0.5	0.3
$a$ ( $\text{m/s}^2$ )	1.6	-1.6	-5
$a_k$ ( $\text{m/s}^2$ )	1.4	-1.4	-4

Table 8 Mean lift, average vertical acceleration computed from Newton's second law,  $a$ , and average vertical acceleration computed from displacement and velocity,  $a_k$ , in one stroke.

As shown in Table 8, the magnitude of ' $a$ ' in the three cases is always larger than ' $a_k$ '.  $a_k$  is 88%, 88% and 82% of  $a$  in the three cases respectively. This verifies the reasonable accuracy of the lift results and the displacement results.

## 5: Left hindwing kinematics

According to the results above, when a forewing is damaged, the corresponding hindwing will become more important for generating lift forces. In this part, left hindwing kinematics in the IW and OFD cases are compared. Since the lift forces of the left hindwing in the OFD case appears to have two peak values during the upstroke (Figure 11 e)), that is, the left hindwing mainly generates lift forces in the upstroke, so the kinematics in the upstroke is examined. Figure 12 shows the trajectory of mid chord of the left hindwing and the variation of the pitching angle in the IW and OFD cases. Figure 12 a) shows that the mean stroke plane angle of the upstroke in the IW case is

larger than the OFD case, and b) displays that the wing pitching angle in the IW case changes from  $81^\circ$  to  $110^\circ$ , but the range of angles in the OFD case is from  $45^\circ$  to  $118^\circ$ . The maximum value of wing pitching angle is the same for the two cases.

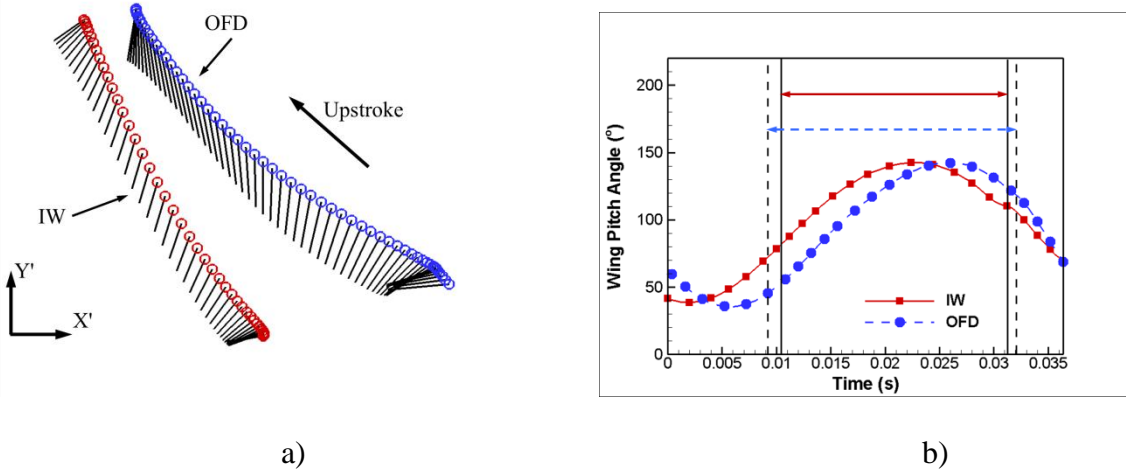


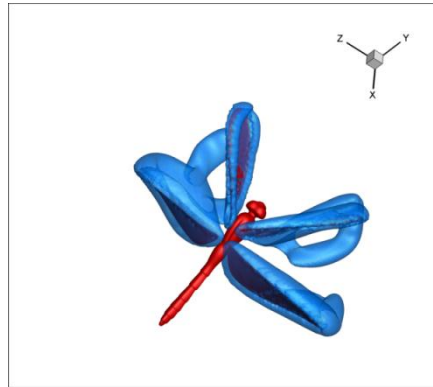
Figure 12 Trajectory of mid chord of the left hindwing and the corresponding instantaneous pitching angle in the IW and OFD cases. a) presents the projection of trajectory of mid chord on X'Y' plane in the left hindwing's upstroke. The circle stands for the leading edge, and the segment stands for mid-chord length project to the X'Y' plane. b) presents the wing pitch angle with respect to the stroke plane for the two cases, and the regions between two solid lines and between two dashed lines are the upstrokes of the left hindwing in the IW and OFD cases respectively.

On the other hand, according to the frequency shown in Table 3, in the IW case, the left wings and the right forewing have similar frequencies in the two complete strokes, but only the right hindwing displays a lower frequency. The dragonfly in the OFD case

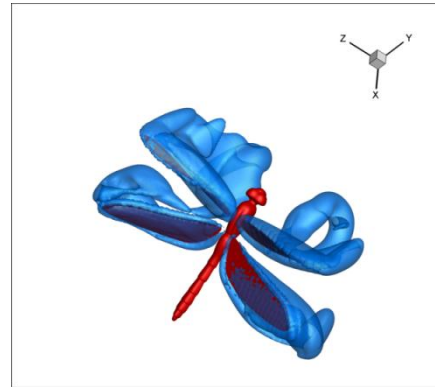
shows similar frequencies on the left wings and the right forewing, while the right hindwing's frequency has an obvious increase from 25.8Hz to 28.2Hz. After 40% of wing area of the two forewings is cut off separately, the frequencies of the two forewings are not changed, but the frequencies of hindwings increase slightly especially in the OFD case.

## 6: Flow features

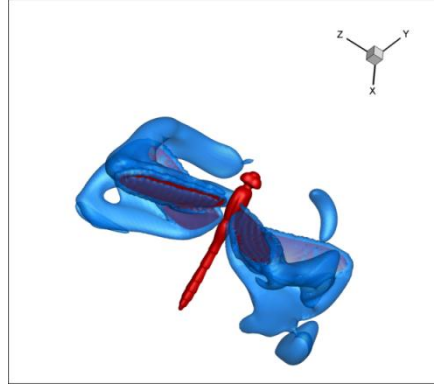
The flow generated by the dragonfly's four wings can show how the lift is being produced. Figure 13, Figure 14, and Figure 15 illustrate the variation of the flow features during the 0.08s for the three cases in different perspective view, respectively. Figure 16 shows the position of the three cases in the side view.



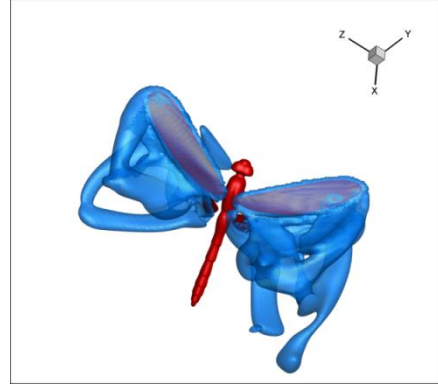
a)  $t = 0.01s$



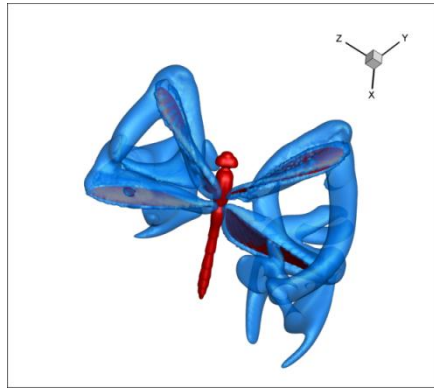
b)  $t = 0.02s$



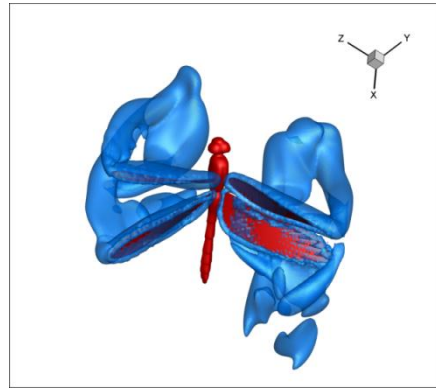
c)  $t = 0.03s$



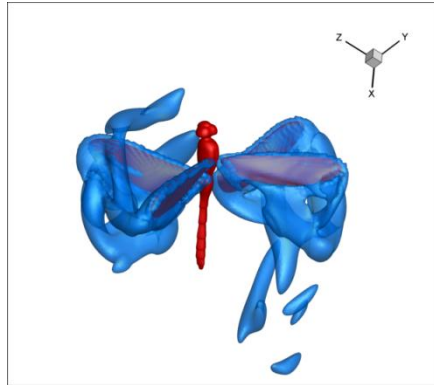
d)  $t = 0.04s$



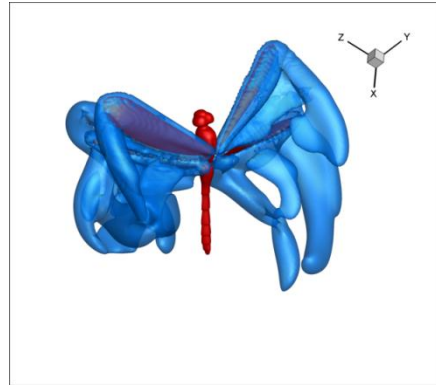
e)  $t = 0.05s$



f)  $t = 0.06s$



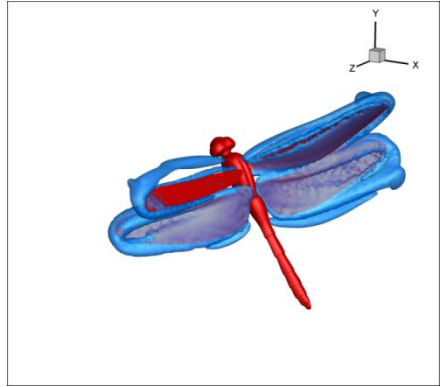
g)  $t = 0.07s$



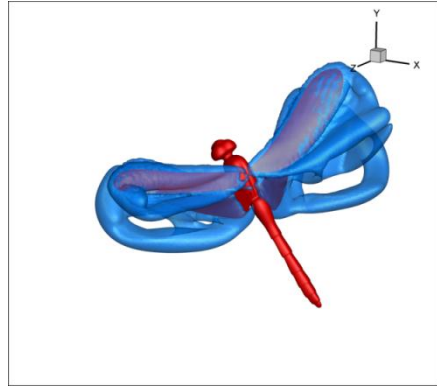
h)  $t = 0.08s$

Figure 13 Flow Feature shed from the intact wings during 0.08s (the IW case).

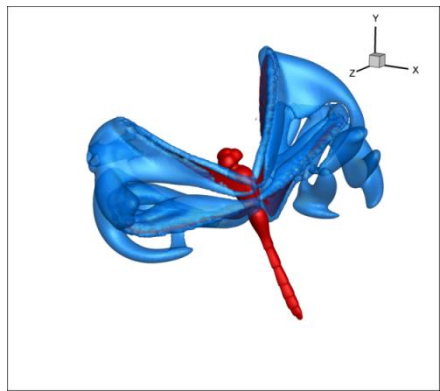
Iso-surface of vorticity  $\lambda_2$  is 3.



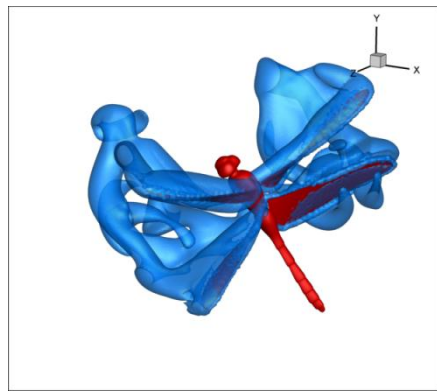
a)  $t = 0.01s$



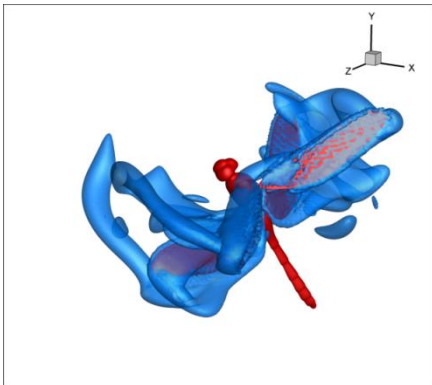
b)  $t = 0.02s$



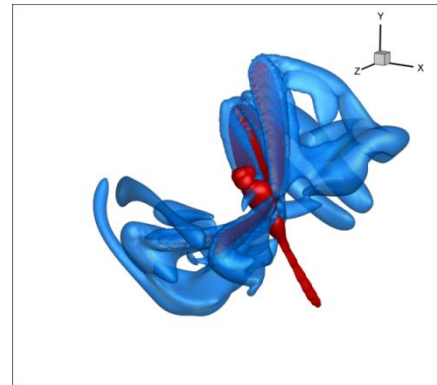
c)  $t = 0.03s$



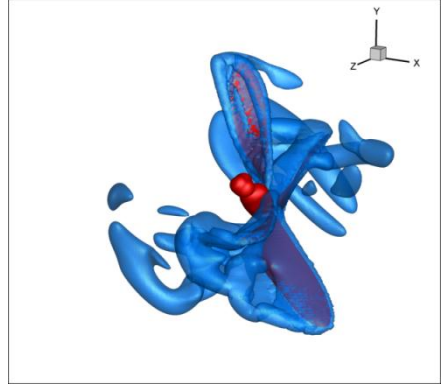
d)  $t = 0.04s$



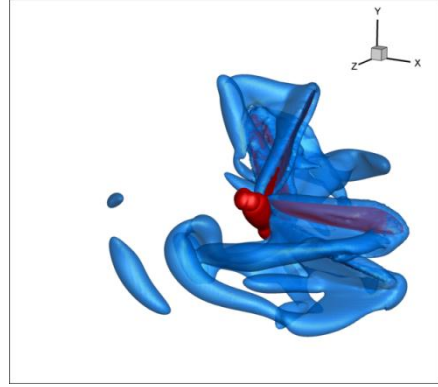
e)  $t = 0.05s$



f)  $t = 0.06s$

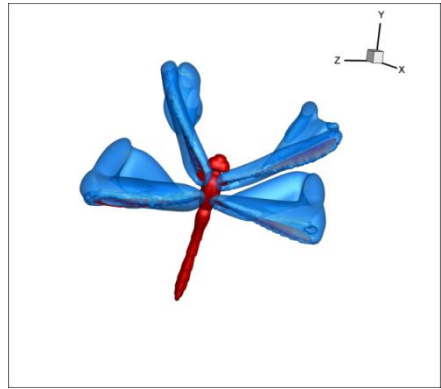


g)  $t = 0.07s$

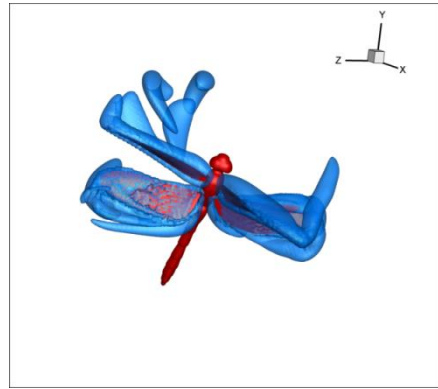


h)  $t = 0.08s$

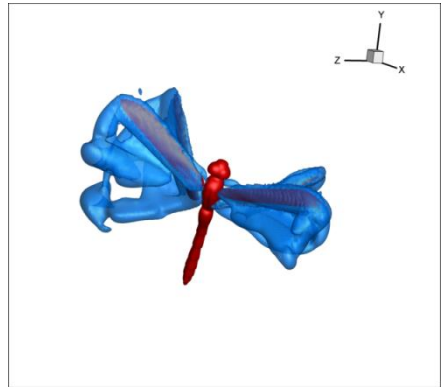
Figure 14 Flow Feature shed from the dragonfly's wings including 40% loss of left forewing area during 0.08s (the OFD case). Iso-surface of vorticity  $\lambda_2$  is 3.



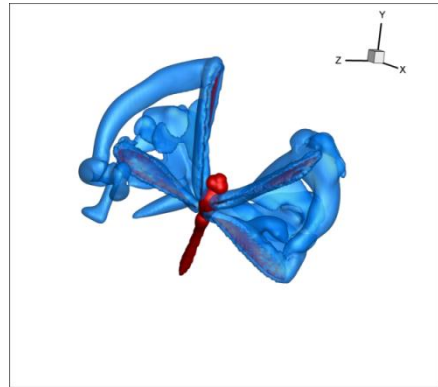
a)  $t = 0.01s$



b)  $t = 0.02s$

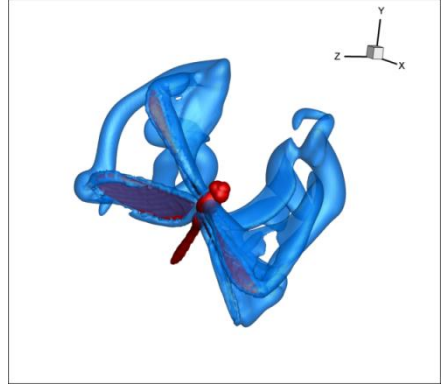


c)  $t = 0.03s$

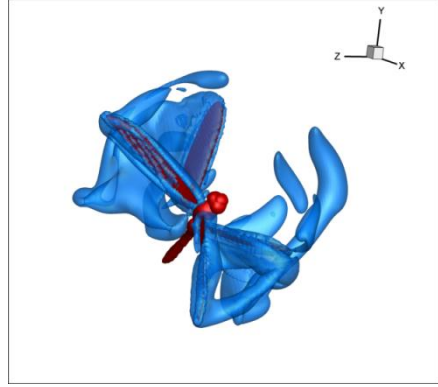


d)  $t = 0.04s$

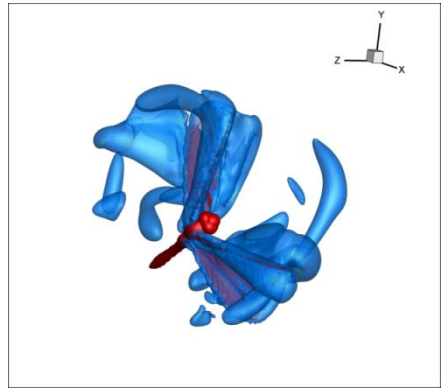




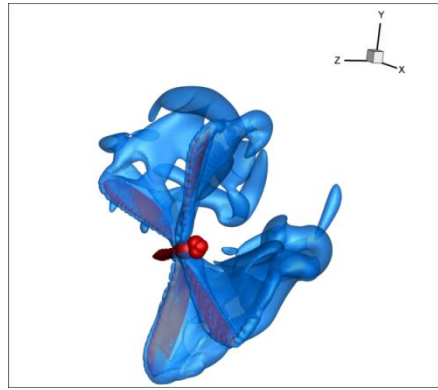
e)  $t = 0.05s$



f)  $t = 0.06s$



g)  $t = 0.07s$



h)  $t = 0.08s$

Figure 15 Flow Feature shed from the dragonfly's wings including 40% loss of wing area on the two forewings during 0.08s (the DFD case). Iso-surface of vorticity  $\lambda_2$  is 3.

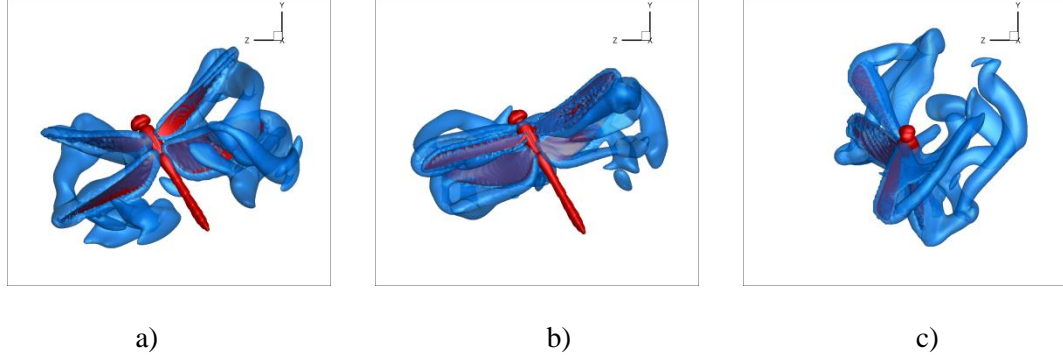
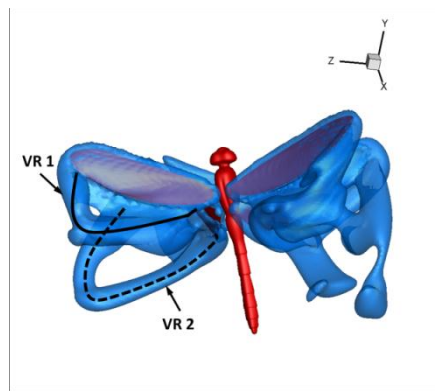


Figure 16 YZ view (side view) of the three cases. a) IW, b) OFD, c) DFD. Iso-surface of vorticity  $\lambda_2$  is 3.

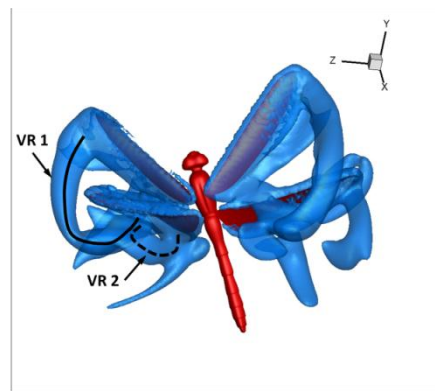
Comparing Figure 13, Figure 14 and Figure 15, the results show that the intact wings always shed a vortex ring (VR) merged with the wing tip vortex (TV) from forewings and hindwings, while the damaged forewing and the intact hindwings could not form VRs especially when the forewings are in the end of upstroke, and the hindwings are in the beginning of downstroke. Also, when the dragonfly is turning right in the DFD case, the interaction between the inner wings is increased. The way that the dragonfly improves the interaction between a forewing and a hindwing is to reduce the distance between them. However, in the OFD case, where the dragonfly is turning left, the interaction between the inner wings is not improved greatly.

Figure 17, Figure 18, and Figure 19 illustrate several specific moments, when the lift forces on the inner wings is the maximum or the minimum, during one stroke to analyze wake structure and its relation with the lift production. Figure 17 shows the flow features generated by the intact wings in the IW case. The reason of discussing lift performance and vortices together is that the variation of lift could be examined by the vortices. For instance, in Figure 17 a), the inner wings produce prominent VRs, VR1 and

VR2, formed by the TV and the starting vortex (the detached trailing-edge vortex) of them respectively. Compared to the Figure 11 a), the vortices at this moment increase the lift forces considerably. At the same time, the lift on the left hindwing also has a small peak. Similarly, since a VR is formed by the TV to trailing-edge vortex (TEV) of the right forewing, it performs an increase of lift force at this period. In Figure 17 b) both the inner wings and the outer wings are producing VRs, especially the VR1 and VR2 on the inner wings are formed by the TV of the left forewing and the TEV detached from the trailing edge of the left hindwing. The VR1 and VR2 help the left hindwing generate lift force. According to the Figure 11 a) the lift force on the left hindwing achieves the maximum at this time, and the lift on the left forewing is also going up slightly. In addition, since the right forewing is experiencing a reversal, the TV is mainly used to help the right hindwing. Simultaneously, the vortices produced by the right hindwing are forming, so the lift from the right hindwing is rising. However, the vertical force on the right forewing keeps decreasing.



a)



b)

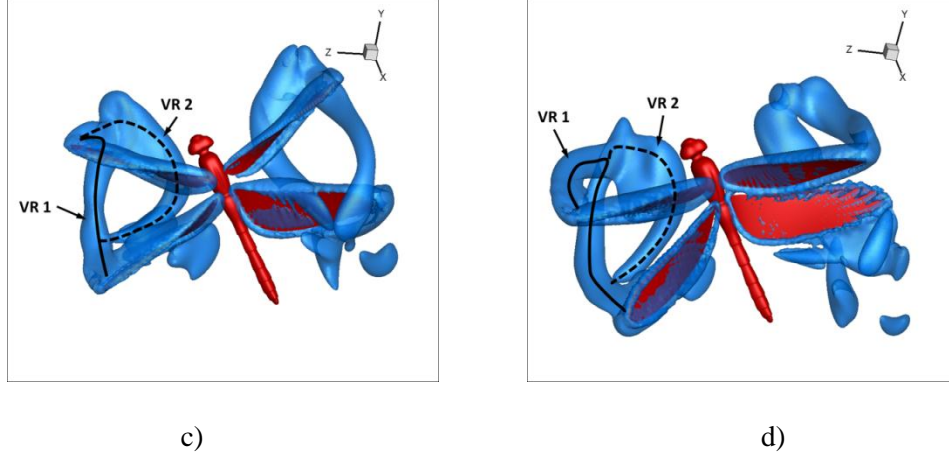


Figure 17 Flow feature of the intact wings in the IW case. a) presents the flow at the big peak of the lift on the left forewing at 0.012s in the downstroke shown in Figure 11 a). b) presents the flow when the right forewing is in the supination, where the left hindwing performs a big lift at 0.018s in Figure 11 a). c) presents the vortices at 0.027s in the upstroke in Figure 11 a) when the left forewing generates the first peak. d) presents the vorticity at 0.034s when the left forewing produces the second peak value in the upstroke in Figure 11 a).

The vortices generated by the four wings during upstroke are shown in Figure 17 c) and d) where the corresponding lift appears the first and second peak value of the left forewing in upstroke in Figure 11 a) respectively. In Figure 17 c), the TV detached from the left hindwing joins the TV and a stopping vortex from the left forewing and forms the VR1 and VR2. Thus, the flow behind the left forewing and the left hindwing is enhanced, and the lift forces on the inner wings are increased which causes the resultant lift to reach a maximum value. Also, if we observe the flow coming from the outer wings, little efficient vortices are shed from the right hindwing since the right hindwing is at reversal. However, some vortices shed from the right hindwing are utilized by the right forewing

so that the vortices around the right forewing keep increasing. The lift generated by the right forewing in Figure 11 b) has an increasing trend. In Figure 17 d), the inner wings and the outer wings have similar flow structure (VR1 and VR2) formed by the TV and the TEV (stopping vortex) of the forewings and the TV of the hindwings. However, since there may be the effect of the wing pitching angle and the phase difference, the lift performance on the different wings are different: the left forewing produces the maximum, while the lift on the right forewing passed the maximum and began to decrease. The hindwings produce increased lift, and the magnitude of lift from both hindwings in the moment of Figure 17 d) is the same ( $0.2 \times 10^{-3}$  N).

In conclusion, the VR formed by the TV and the TEV of the forewings and the TV of the hindwings could influence the lift performance of the forewings and the hindwings. Also, a stopping vortex shed from the trailing edge of the forewings may help the paired hindwings to generate lift forces. Finally, even if the wake structure is similar, the lift performance could be significantly different since the wing pitching angles and the phase difference may also affect the lift performance.

Figure 18 shows the vorticity when the left hindwing produces the maximum or the minimum lift force in the OFD case. Figure 18 a) presents the moment when the left hindwing produces the biggest lift in the downstroke shown in Figure 11 c). The left hindwing generates a large leading-edge vortex (LEV), and then this vortex sheds from the wing tip and joins the starting vortex to forms the VR2 which can help increase lift. At this time, the left forewing generates the VR1 using the same strategy, and these VRs are very similar to the structure shown in Figure 17 a). However, the lift generated by the left forewing in the OFD is not increased as in the IW case. Figure 18 b) illustrates the

flow structure when the resultant lift of the inner wings is maximum in Figure 11 c). The TV shed from the left forewing is merged with the TV of the left hindwing to form the VR1, which increases the lift performance of the left hindwing. Also, since the VR1 is growing, the lift on the left forewing is also increasing. However, the vorticity of the outer wings in Figure 18 b) is decomposed, where the right forewing is in supination. Therefore less LEV on the right forewing is produced, and the lift generated by the outer wings drops.

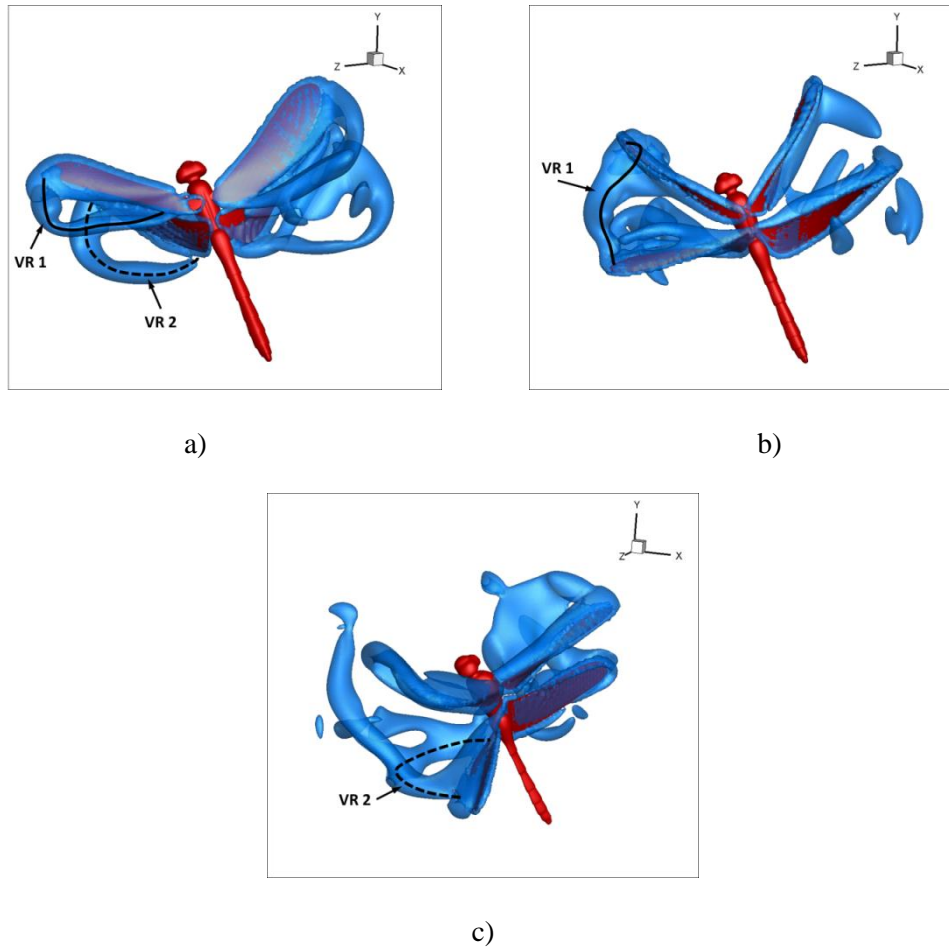


Figure 18 Flow feature of four wings including damaged left forewing in the OFD case. a) presents the flow feature when the lift generated by the left hindwing is the maximum at 0.014s in the downstroke in Figure 11 c). b)

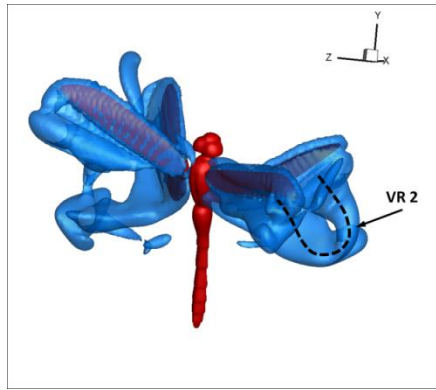
presents the flow feature when the maximum lift is generated by the left hindwing at 0.023s in the upstroke in Figure 11 c). c) presents the vorticity when the minimum lift is generated by the left hindwing at 0.033s in the upstroke in Figure 11 c).

Figure 18 c) shows that the TV shed from the left hindwing cannot join the detached vorticity from the damaged left forewing since the vortex shed from the left forewing is less than that of an intact forewing. That is, the 40% loss of wing area does impact the formation of wings' VR negatively. Since the vorticity from the damaged left forewing cannot be utilized to enhance the vortices from the left hindwing in the downstroke of the forewing, the lift drops evidently. The VR2 formed by the TV and the TEV of the left hindwing is maintained. However, the left forewing is not affected since the VR is nearly parallel to the horizontal surface which can prominently increase the lift performance. On the other hand, the vortices shed from the outer wings merge together. The vertical force generated by the right hindwing increases slightly, while the force from the right forewing decreases.

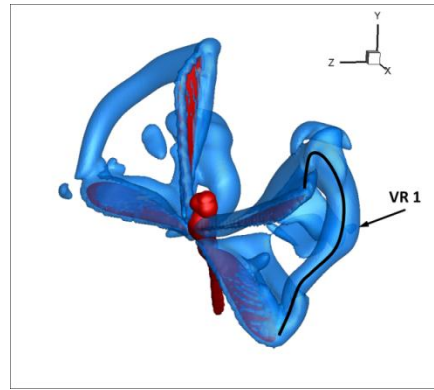
In conclusion, after the left forewing is cut, the vortices are reduced, and the interaction of the vorticity between the left forewing and left hindwing is decreased compared the IW and OFD cases.

Figure 19 shows the vorticity in the DFD case in terms of the maximum or minimum lift force generated by the inner wings. Figure 19 a) displays that only the right hindwing produces a VR (VR2) formed by the TV and the TEV (starting vortex), and hence only the lift on the right hindwing has a peak value (in Figure 11 e) and f)). Figure 19 b) shows that the TV and the TEV (stopping vortex) of the right forewing join the TV

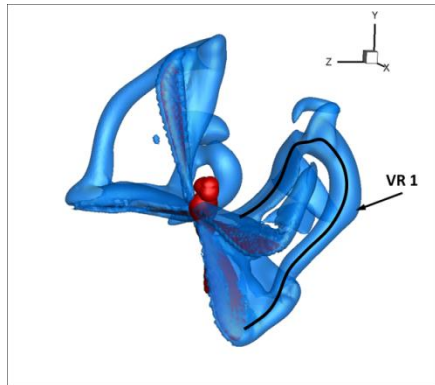
detached from the right hindwing and form the VR1. The outer wings also generate the same VR. However, the TEV shed from the right forewing is stronger than the left forewing because the TEV of the left forewing has been detached and shed while the right forewing is maintaining the TEV. Owing to this distribution of the wake structure, the right hindwing is producing the largest lift value, while the force produced by the left hindwing reduces. The lift generated by the forewings is increasing. Also, at this moment, the vortices generated by the inner wings are stronger than the outer wings, and TEV shed from the right forewing is trying to merge with the right hindwing.



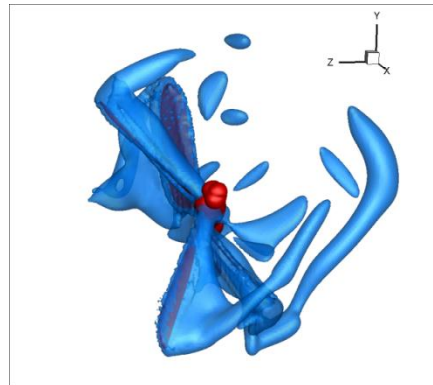
a)



b)



c)



d)



Figure 19 Flow feature of the four wings in the DFD case. a) presents the vorticity in terms of the first peak value of the lift generated by the right hindwing at 0.008s in the downstroke shown in Figure 11 f). b) presents the vortices in terms of the biggest lift generated by the right hindwing at 0.023s in the upstroke shown in Figure 11 f). c) presents the flow when the lift generated by the right forewing is the maximum in the upstroke at 0.027s in Figure 11 f). d) presents the vorticity when the lift generated by the right hindwing is minimum in the upstroke at 0.034s in Figure 11 f).

Figure 19 c) illustrates that the TV shed from the right forewing cannot connect to either the TEV of the right forewing, or the TV detached from the right hindwing. However, the TEV of the right forewing joins the TV of the right hindwing and forms the VR1. The TVs of the outer wings are connected, and the TEV (stopping vortex) of the left forewing enhances the VR. In contrast, the TEV of the left hindwing is not utilized. The vorticity from the inner and the outer wings shows that the resultant lift on the right side is bigger than the left side, which exactly matches the quantitative lift shown in Figure 11 e) and f). Figure 19 d) shows the flow structure at the end of the upstroke of the right forewing when the hindwings are starting downstroke. There is no VR from the two paired wings at this time. The right hindwing does not produce any efficient vortex, so the lift drops to a minimum and becomes resistive. The TEV and the TV shed from the right forewing are stronger than the left forewing, so the lift from the former is starting to increase while the lift generated by the latter keeps decreasing. Also, because of the damaged forewings, the wake structure at this moment is not effective in producing lift.

Also, the forewings and hindwings do not have as much interaction as the intact forewings and hindwings.

Comparing Figure 17, 18 and 19, the VR1 which stands for the combination of the TV shed from the wings at the same side always exists in the IW case. However, after the left forewing or double forewings are damaged, the VR1 in the upstroke of the forewing could not be formed anymore. In order to study this phenomenon, the vortex around 75% of the inner forewing's leading edge from the wing root is studied. Figure 20 shows the sliced vorticity on the inner forewing at the end of the downstroke.

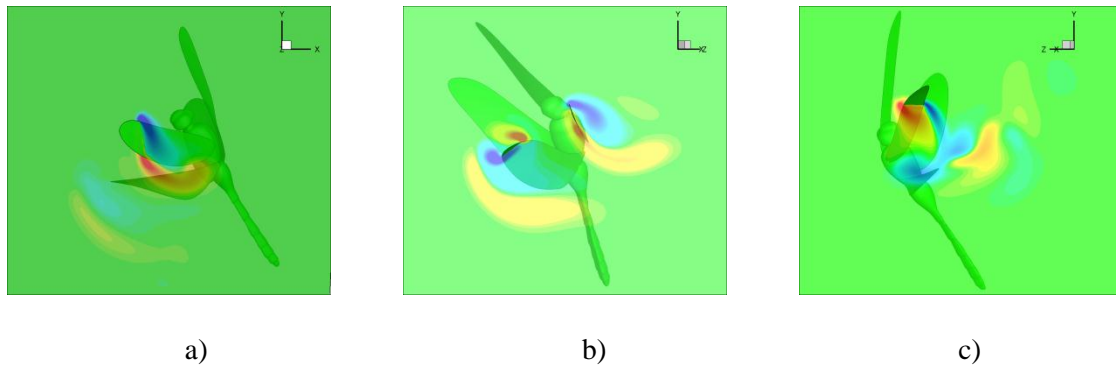


Figure 20 Comparison of the vorticity slice of the inner forewing at the end of downstroke. a) presents the vortex around the left forewing in the IW case. b) presents the vortex near the damaged left forewing in the OFD case, and the vortex at the left side is produced by the left hindwing. For the vortex generated by the left forewing in a) and b), the blue area stands for the LEV, and the red and yellow area stands for the TEV. c) presents the vortex generated by the damaged right forewing in the DFD case. The red area stands for the LEV, and the blue area stands for the TEV since the motion of the dragonfly with two-sided forewing damage is right turn different from the IW and OFD cases.

Comparing the three cases in Figure 20, the LEV generated by the damaged forewing sheds along the chord before it goes to the wing tip along the leading edge. That is, the TV of the damaged wing is weakened, and the LEV becomes unstable due to the increase of the aspect ratio (results from the reduced wing area). This instability directly results in the disappearance of the tip vortex ring (VR1) in the upstroke of the forewings, and the aerodynamic performance is also reduced.

## IV. CONCLUSIONS

From 10 July to 31 August in 2011, 15 dragonflies, *Eastern Pondhawk* (*Erythemis simpliciolis*), were captured from the pond of Nutter Center in Wright State University and were filmed in high-speed photogrammetry laboratory to study the effect of wing damage on their free flight of takeoff maneuver. This experiment aims to investigate the effect of cutting the forewings along wing span. A specific case wherein the dragonfly lost approximately 40% of forewing area along span was selected to study the effect of forewing area removal on aerodynamic performance. Its morphological parameters including mass, wing chord length, wing span length, and wing beat frequency were recorded for each wing.

After clear images were filmed, three-dimensional surface reconstruction technology (using Autodesk MAYA) is introduced to reconstruct the flight motion and obtain raw data about wings and body motion. Then the *PiCar3D* solver is utilized to perform a direct numerical simulation to acquire vortices around wings along with forces generated by wings. Results in this thesis consist of displacement of center of mass, resultant lift force during two strokes, the time-average lift forces in one stroke, time history of lift forces in one stroke, hindwing kinematics, and near-field vorticity distribution. Results show that:

- The dragonfly with double-side forewing damage (DFD) performs the worst in terms of vertical displacement comparing to single-left-forewing damage (OFD) and intact wings (IW);

- Mean lift produced by the four wings in the OFD and DFD cases is less compared to the IW case. This value in the downstroke of forewings is reduced when compared to the upstroke of forewings in wing damage cases. Especially in the DFD case, mean total lift in the downstroke is negative.
- In takeoff motion, there is no evidence that the most lift is generated in the downstroke, whereas in the OFD and DFD cases most lift forces are generated in the upstroke;
- The lift force generated by the outer wings is larger than or equal to that produced by the inner wings during downstroke of forewings, but the outer wings' lift production becomes smaller than the inner wings' during upstroke;
- When a forewing is damaged, the hindwing at the same side plays a dominant role in producing lift;
- Span-wise forewing area removal reduces forewing tip vorticity since the increase of aspect ratio results in shedding of the leading edge vortex along chord.
- The decreased tip vorticity leads to the detachment of the tip vortex ring during upstroke.

## V. FUTURE WORK

Currently, we have investigated the aerodynamic effect of forewing damage on dragonflies' takeoff motion which mainly focuses on lift performance and vortex variation. During the 0.08s studied, the dragonfly turns left ( $90^\circ$ ) in the IW case; it turns left ( $90^\circ$ ) in the case of OFD; while the DFD case turns right ( $180^\circ$ ). Since the turning motion of the three cases selected in this thesis is different, the effect of damaged forewings on maneuverability might have an obvious difference. The following portions will be examined to compare maneuverability:

- The variation of forces and moments on the horizontal surface due to one-sided or two-sided forewing damage.
- The relationship between near-field vorticity and horizontal forces, and its effect on maneuverability.

Also, the same dragonfly with left forewing area removal which has a takeoff motion with  $180^\circ$  right turn will be studied in the future. However, the most difficult part of this study is to define wing kinematics for dragonflies' takeoff maneuver in this extremely complicated free flight mode. Even so, wing kinematics of dragonflies' free flight is going to be the focus. If the difference of angle of attack between intact wings and damaged wings can be obtained, it will provide a better understanding on the variation of aerodynamic performance.

## REFERENCES

1. Aono, H., F. Liang, and H. Liu, *Near- and far-field aerodynamics in insect hovering flight: and integrated computational study*. J. Exp. Biol. 2008. 211: p. 239-257.
2. Cartar, R.V., *Morphological senescence and longevity - an experiment relating wing wear and life-span in foraging wild bumble bees*. Journal of Animal Ecology, 1992. 61(1): p. 225-231.
3. Combes, S.A., J.D. Crall, and S. Mukherjee, *Dynamics of animal movement in an ecological context: dragonfly wing damage reduces flight performance and predation success*. Biology Letters, 2010. 6(3): p. 426-429.
4. Combes, S.A., J.D. Crall, and S. Mukherjee, *Wing damage and flight performance in dragonflies: effects of area loss on force production and aerial predation*. Integrative and Comparative Biology, 2010. 50: p. E33-E33.
5. Dickinson, M., *The effects of wing rotation on unsteady aerodynamic performance at low Reynolds numbers*. J. Exp. Biol. 1994. 192: p. 179-206.
6. Dickinson, M.H. and K.G. Götz, *Unsteady aerodynamic performance of model wings at low Reynolds numbers*. J. Exp. Biol. 1993. 174: p. 45-64.
7. Dong, H. Koehler, C. Liang, Z. Wan, H., and Gaston, Z. *An Integrated Analysis of a Dragonfly in Free Flight*. 40th AIAA Fluid Dynamics Conference and Exhibit 2010. 2010-4390.

8. Dukas, R. and L. Dukas, *Coping with nonrepairable body damage: effects of wing damage on foraging performance in bees*. *Animal Behavior* 2011. 81(3): p. 635-638.
9. Ellington, C. P. *The aerodynamics of hovering insect flight. II. Morphological parameters*. *Phil. Trans. R. Soc.* 1984a. Lond. B 305, 17–40.
10. Ellington, C. P. *The aerodynamics of hovering insect flight. III. Kinematics*. *Phil. Trans. R. Soc.* 1984b. Lond. B 305, 41–78.
11. Ellington, C. P. *The aerodynamics of hovering insect flight. V. A vortex theory*. *Phil. Trans. R. Soc.* 1984c. Lond. B 305, 115–144.
12. Ellington, C. P. *The aerodynamics of hovering insect flight. VI. Lift and power requirements*. *Phil. Trans. R. Soc.* 1984d. Lond. B 305, 145–181.
13. Foster, D.J. and R.V. Cartar, *Wing wear affects wing use and choice of floral density in foraging bumble bees*. *Behavioral Ecology*, 2011. 22(1): p. 52-59.
14. Mittal, R., H. Dong, M. Bozkurttas, F. M. Najjar, A. Vargas, and A. von Loebbecke, *A versatile sharp interface immersed boundary method for incompressible flows with complex boundaries*. *Journal of Computational Physics* 2008. 227: p. 4825-4852.
15. Sane, S.P. and M.H. Dickinson, *The control of flight force by a flapping wing: lift and drag production*. *J Exp Biol*, 2001. 204 (Pt 15): p. 2607-26.
16. Taira, K., and T. Colonius, *Three-Dimensional Separated Flows Around Low-Aspect-Ratio Flat Plates*. *Journal of Fluid Mechanics* 2009 623: p. 187–207.



17. Wakeling, J.M., and C. P. Ellington, *Dragonfly flight. III. Lift and power requirements*. J Exp Biol, 1997. 200: p. 583-600